

Large (and Deep) Factor Models

Bryan Kelly, Boris Kuznetsov, Semyon Malamud, and Teng Andrea Xu*

February 13, 2024

Abstract

We open up the black box behind Deep Learning for portfolio optimization and prove that a sufficiently wide and arbitrarily deep neural network (DNN) trained to maximize the Sharpe ratio of the Stochastic Discount Factor (SDF) is equivalent to a *large factor model (LFM)*: A *linear* factor pricing model that uses many non-linear characteristics. The nature of these characteristics depends on the architecture of the DNN in an explicit, tractable fashion. This makes it possible to derive end-to-end trained DNN-based SDFs in closed form for the first time. We evaluate LFMs empirically and show how various architectural choices impact SDF performance. We document *the virtue of depth complexity*: With enough data, the out-of-sample performance of DNN-SDF is increasing in the NN depth, saturating at huge depths of around 100 hidden layers.

1 Introduction

We live in the era of deep learning. The remarkable success of artificial intelligence algorithms in image recognition, natural language processing, drug, and mineral discovery (Jumper et al., 2021; Merchant et al., 2023) (to name a few) can be largely attributed to the surprising ability of deep neural networks (DNNs) to learn intricate non-linearities in the data. Finance

*Bryan Kelly is at Yale School of Management, AQR Capital Management, and NBER; www.bryankellyacademic.org. Boris Kuznetsov is at the Swiss Finance Institute, EPFL. Semyon Malamud is at the Swiss Finance Institute, EPFL, and CEPR and is a consultant to AQR. Teng Andrea Xu is at EPFL. Semyon Malamud gratefully acknowledges the financial support of the Swiss Finance Institute and the Swiss National Science Foundation, Grant 100018_192692. AQR Capital Management is a global investment management firm that may or may not apply similar investment techniques or methods of analysis as described herein. The views expressed here are those of the authors and not necessarily those of AQR. This work was supported by a grant from the Swiss National Supercomputing Centre (CSCS) under project ID sm81. We thank Mohammad Pourmohammadi for his excellent comments and suggestions.

is no exception. A quickly growing number of papers show how NNs with astronomical numbers of estimated parameters can produce return predictions, optimal portfolios, and stochastic discount factors (SDF) that strongly dominate simpler, parsimonious models. Recent theoretical results (Kelly et al., 2022; Didisheim et al., 2023) attribute the success of NNs to the *virtue of complexity*: The fact that the out-of-sample performance monotonically increases with the number of model parameters; or, in simple terms: “bigger models are always better.” Yet, the picture drawn by the data is much more subtle. Deeper NNs do not always perform better than shallow ones, and our understanding of the underlying mechanisms is still in its infancy.¹

Most finance academics view DNNs as a “black box” with an incomprehensible ability to select optimal portfolios and SDFs based on opaque gradient descent algorithms. Since the objective function (the Sharpe ratio) is highly non-concave with respect to the DNN coefficients (the neural weights and biases) and has a tremendous number of local minima, it is striking that the DNN can select “good” local minima that work out-of-sample. This paper aims to open up the black box underlying the DNN-based SDFs and show exactly what a DNN-SDF learns in the limit when the underlying network becomes wide.

Our analysis relies heavily on the recent Neural Tangent Kernel (NTK) discovery by (Jacot et al., 2018). Namely, (Jacot et al., 2018) show that the prediction of a wide NN trained to minimize mean squared error (MSE) by gradient descent with a sufficiently small learning rate (i.e., small descent steps) converges to that of kernel regression,² with a particular kernel, the NTK, that can be computed explicitly from the NN architecture and the distribution from which NN weights and biases are initialized.³

Leveraging the powerful machinery of (Jacot et al., 2018), we prove an analogous result for the NN trained to maximize the SDF Sharpe ratio. We show that the DNN-SDF can also be characterized in terms of an explicit kernel that we name the *Portfolio Tangent Kernel (PTK)*. Strikingly, while the DNN-SDF is highly non-linear, we show that it admits a representation as the Markowitz portfolio of characteristics-based factors in the limit as the number of these factors grows indefinitely. The underlying characteristics absorb the structure of the DNN in an explicit (but complex) fashion. We call such a representation a Large Factor Model (LFM).

Our closed-form solution for the DNN-SDF sheds light on some important and puzzling phenomena underlying deep learning. First, why does depth even matter? After all, even shallow models have the *universal approximation property*: Any continuous function can

¹See, e.g., (Lee et al., 2020).

²While the optimized objective does have a huge number of local extrema, they depend on the weight initialization in a simple, linear fashion that can be described analytically.

³(Yang, 2020) extended their results to arbitrary NN architectures.

be approximated by a single-hidden-layer NN. More generally, any rich parametric family of functions should perform equally well in the task of approximating the underlying true, unobservable SDF. The reality, however, is much more subtle. What matters is the ability of the particular function family to learn the ground truth *using a limited amount of training data*. This ability is linked to the *alignment* of the data-generating process with the *inductive biases* of the particular function family and defines *limits to learning*, characterized for factor SDFs in (Didisheim et al., 2023). When the inductive bias expressed by DNN is better aligned with the data than the bias expressed by the shallow net, the deep net will outperform.⁴ The explicit representation of a DNN-SDF as an LFM makes it directly amenable to the theoretical analysis of factor-based SDFs in (Didisheim et al., 2023). In particular, we can analytically compute the *implicit regularization* of the LFM using the eigenvalue decomposition of the factor covariance matrix.

Second, our analysis relies heavily on the analytical characterization of the gradient descent dynamics. We show how the *learning rate* of the gradient descent and the associated early stopping (the fact that, in the real world, we can only perform a finite number of gradient descent steps) strongly impact the DNN-SDF. We show analytically how a smaller learning rate acts as a regularization parameter analogous to the ridge penalty of the ridge regression. Choosing the optimal learning rate thus amounts to a spectral shrinkage of the covariance matrix, making DNN-SDFs amenable to modern spectral shrinkage techniques (Kelly et al., 2023b). These results link our analysis to the recent discoveries in the theory of DNNs (Zhou et al., 2023), showing how the choice of the learning rate and, more generally, the learning algorithm itself (e.g., Stochastic Gradient Descent; Adam of (Kingma and Ba, 2014); etc.) might drastically impact the out-of-sample performance of DNNs: *Different algorithms converge to different local minima with drastically different out-of-sample behavior*. In short, both the function family and the training algorithm matter a lot for the performance of DNNs.

Our main theoretical finding is that computing the DNN-SDF is equivalent to running a kernel ridge version of the maximal Sharpe ratio regression of (Britten-Jones, 1999a) with a special kernel discovered in our paper, the PTK. If we wanted to solve a standard return prediction problem in such a kernel setting, we would need to deal with ultra-high-dimensional kernel matrices of dimensions $(N \cdot T) \times (N \cdot T)$, where N is the number of stocks and T is the number of in-sample time periods. By contrast, the PTK kernel matrix is T -dimensional. We leverage recent advances in the numerical algorithms for computing NTK (Novak et al., 2019) to develop a simple procedure for computing PTK. It allows us to work with very large panel datasets.

⁴See, also, (Ghorbani et al., 2020).

We use our closed-form solutions to address a key question: What is the role of depth in DNN-SDFs? Strikingly, despite the existence of a very large number of asset pricing and portfolio optimization papers utilizing deep learning methods, none of them actually study deep neural nets; Instead, they use DNNs with five hidden layers at most. This approach, motivated by attempts to avoid overfitting, contradicts the one exploited by real-world DNN applications that use nets with hundreds, if not thousands, of hidden layers. Our results allow us to study such extremely deep DNNs. As in (Didisheim et al., 2023), we use monthly stock characteristics data from (Jensen et al., 2023). We train our DNNs using a grid of rolling windows, from very short (one year) to relatively long (10 years). We find that exploiting depth consistently is only possible with enough data. For shorter rolling windows, shallow models often perform better out-of-sample. By contrast, for longer windows, the model has enough data to detect subtle non-linearities hidden in the inductive bias of the very deep neural nets.⁵ We document the *the virtue of depth complexity*: The OOS Sharpe ratio and the model alpha are both monotone increasing in the network depth, sometimes saturating at around 30 hidden layers. This finding reinforces the key point discussed above: The performance of an ML model depends on its ability to learn from limited amounts of data; DNNs require more data to learn more intricate patterns. Yet, as (Didisheim et al., 2023) show, due to limits to learning, both shallow and deep models will only learn highly imperfect approximations to the ground truth, and these approximations might even be entirely orthogonal, as recent evidence (Kelly et al., 2023a) suggests.

We also study the role of parameter initialization, an important aspect of neural network architecture that is usually ignored in most studies of DNNs. We show analytically how this initialization impacts PTK as a form of smart, layer-wise bandwidth for the kernel and use these insights to develop better initializations and show how this could significantly improve performance.

2 Literature Review

The economic doctrine of sparsity dictates the search for an SDF based on a small number of factors. Yet, an emergent literature documents that richly parameterized SDFs strongly dominate their sparse counterparts. See, e.g., (Cochrane, 2011), (Moritz and Zimmermann, 2016), (Harvey et al., 2016), (McLean and Pontiff, 2016), (McLean and Pontiff, 2016), (Kelly et al., 2020), (Feng et al., 2018), (Chen et al., 2023), (Chinco et al., 2019), (Han et al., 2019),

⁵If the data were entirely stationary, then more data (longer training window) would always be better. However, in reality, data is non-stationary, introducing a subtle tradeoff. The model needs to choose between being more reactive to changing market regimes and using more data to reduce estimation noise. Investigating this tradeoff is an important direction for future research.

(Chen et al., 2023), (Gu et al., 2020a), (Hou et al., 2020), (Feng et al., 2020), (Kozak et al., 2020a), (Bryzgalova et al., 2020), (Gu et al., 2020b), (Andreini et al., 2020), (Dixon and Polson, 2020), (Freyberger et al., 2020), (Avramov et al., 2023), (Guijarro-Ordóñez et al., 2021), (Preite et al., 2022), (Jensen et al., 2023), (Giglio et al., 2022), (Leippold et al., 2022), (Filipović and Pasricha, 2022), (Didisheim et al., 2023), Simon et al. (2022), Kozak (2020), (Kelly et al., 2023a), (Feng et al., 2023), and (Kelly and Xiu, 2023) for a recent survey.

All these papers find evidence for a very rich and highly non-linear conditional structure in stock returns. Such a structure requires tools for building conditional SDFs that efficiently learn and incorporate information in stock characteristics. A conventional way of building such conditional SDFs is to first construct characteristics-based factors based on many linear (or non-linear) characteristics and then build an unconditionally efficient portfolio from these factors. In this paper, we refer to such an SDF as an (unconditional) *factor model*. With some shrinkage, this approach can be very powerful (Kozak et al., 2020b; Kelly et al., 2023b) even with simple linear characteristics from the standard factor zoo. However, as (Kozak and Nagel, 2023a) argue, one might need many characteristics-based factors to approximate the SDF properly. (Didisheim et al., 2023) formalize this intuition and prove the long-standing conjecture that, indeed, in the limit of a large number of characteristics-based factors, an unconditional SDF built from these factors indeed converges to the true, conditional SDF.⁶ That is, one can use *Large Factor Models (LFMs)* to build the true, conditional SDF.

While being highly attractive in terms of their approximation capacity, LFMs naturally face a very serious obstacle: They exhibit enormous statistical complexity and require the estimation of a very large number of parameters (factor weights in the SDF), far exceeding the number of observations. Intuitively, one might thus expect that a parsimonious version of the LFM might do better out-of-sample because it significantly reduces the in-sample overfit.⁷ (Didisheim et al., 2023) prove that this intuition is wrong. Based on the discoveries in (Kelly et al., 2022), (Didisheim et al., 2023) establish the *virtue of complexity in factor pricing models*. Namely, higher-dimensional, extremely richly parametrized LFMs perform better out-of-sample. These models leverage tens of thousands of nonlinearities hidden in the relationship between characteristics and stock returns.

The model of (Didisheim et al., 2023) is equivalent to a shallow but wide, single-hidden-layer NN where *the weights in the hidden layer are not optimized* (untrained in the jargon of

⁶Formally, building the SDF requires the true conditional covariance matrix of stock returns. However, this matrix is unobservable and impossible to recover in small samples. (Didisheim et al., 2023) show that with a complex model, the best portfolio available to an investor need not estimate the conditional covariance matrix of returns at all. Instead, the investor needs only find the *unconditionally optimal* portfolio of factors.

⁷Indeed, the in-sample Markowitz portfolio of P factors based on T observed achieves an infinite in-sample Sharpe ratio whenever $P > T$.

Machine Learning (ML)).⁸ This makes it difficult to compare their results with other NN-based SDF models in the literature that typically use deeper but narrow NN architectures. Furthermore, most papers in this literature train all weights of the NN (the so-called end-to-end training), including those in all hidden layers. For example, (Gu et al., 2020b) use the classical DNN architecture with four hidden layers with 32, 16, 8, and 4 neurons; (Chen et al., 2023) use a four-layer network with 64 neurons in each layer, and (Fan et al., 2022) use a 4-layer neural network with four neurons in each layer. Such narrow network architectures are still richly parametrized and operate in a regime that is close to overfit, as can be seen from very large differences in their in- and out-of-sample performance, documented in the above-mentioned papers. This makes them extremely difficult to study analytically: Their loss landscape is already highly non-convex, with numerous local minima and uncertain out-of-sample performance. By contrast, in this paper, we study wide neural nets of arbitrary architecture. Contrary to (Didisheim et al., 2023), our nets are fully trained, including all weights in all hidden layers. Yet, they are analytically tractable due to the Neural Tangent Kernel (NTK) technology from (Jacot et al., 2018). We derive our conditional DNN-SDF in closed form and study its properties and the dependence on depth, including very deep neural architectures with more than a hundred hidden layers. Strikingly, we find that deep nets are able to find more subtle non-linearities as we increase depth, exhibiting high excess returns relative to the (already complex) shallow models of (Didisheim et al., 2023). It would be very interesting to understand the relationship between narrow nets of (Gu et al., 2020b; Chen et al., 2023; Fan et al., 2022; Simon et al., 2022) and wide neural nets of our paper and see whether the virtue of complexity (a monotone increase of the Sharpe Ratio in the width of the network) holds for DNNs. We leave this as an important direction for future research. Finally, we note that our paper focuses on the infinite-width limit of NNs under the so-called standard parametrization. Modern neural nets (such as those used for image recognition and natural language processing) indeed use very wide architectures, sometimes with thousands of neurons in each layer. See, e.g., (Kelly et al., 2023a). However, it is now well understood that other parametrizations might better reflect the behavior of such ultra-complex networks (Yang and Hu, 2021; Yang et al., 2023). Under such alternative parametrizations, the NTK no longer accurately describes DNN behavior. Investigating the role of these parametrizations for DNN-SDFs is an important direction for future research.

⁸Kozak (2020) studies a closed-form kernel SDF formulation, but does not analyze its theoretical properties like Didisheim et al. (2023) or this paper.

3 Parametric SDFs, Kernels, and Neural Networks

We consider a panel dataset of stocks indexed by $i = 1, \dots, N_t$, with excess returns $R_{t+1} = (R_{i,t+1})_{i=1}^{N_t}$ at time $t + 1$. Each stock is equipped with a vector $X_{i,t} = (X_{i,t}(k))_{k=1}^d$ of d characteristics, and we use $X_t = [X_t(1), \dots, X_t(d)] \in \mathbb{R}^{N_t \times d}$ to denote all these characteristics, assembled into a matrix. The true tradable stochastic discount factor (SDF) is given by

$$M_{t+1} = 1 - \pi'_t R_{t+1}, \tag{1}$$

where π_t is the conditionally efficient portfolio

$$\pi_t = E_t[R_{t+1}R'_{t+1}]^{-1} E_t[R_{t+1}], \tag{2}$$

solving

$$\max_{\pi_t} E_t[\pi'_t R_{t+1} - 0.5(\pi'_t R_{t+1})^2]. \tag{3}$$

If X_t encompasses all relevant conditioning information, then π_t in (2) is given by

$$\pi_t = \pi(X_t) \tag{4}$$

for some unknown, potentially highly non-linear function $\pi(X)$. A standard approach to the problem of estimating $\pi(X)$ is to specify a simple, parametric family of functions $f(x; \theta)$ and then use statistical inference to estimate θ . One natural approach is to find θ by maximizing the in-sample analog of the (3) objective. Here, we follow (Didisheim et al., 2023) and consider the ridge-penalized version of this objective:

$$\min_{\theta} L(\theta), \text{ where } L(\theta) = \left(\frac{1}{T} \sum_{t=1}^T (1 - f(X_t; \theta)' R_{t+1})^2 + z \|\theta\|^2 \right), \tag{5}$$

where z is the ridge penalty, serving as a regularization. Similarly to (Britten-Jones, 1999b) and (Didisheim et al., 2023), the optimal parametric portfolio return $f(X_t; \theta)' R_{t+1}$ solving (5) is optimized in-sample to behave as close as possible to a positive constant (with respect to the in-sample mean squared error), subject to a penalty for the weight vector θ . By direct calculation, this is equivalent to finding the parametric portfolio with the highest in-sample Sharpe ratio up to the ridge penalty term. (Kelly and Xiu, 2023) dub this “maximum Sharpe ratio regression” (or MSRR) and argue that it is the natural objective for ML-based SDF estimation problems.

Formally, with enough data (i.e., a very large T), any sufficiently expressive function family $f(x; \theta)$, $\theta \in \mathbb{R}^P$, can be used to approximate the $\pi(x)$ in (4) arbitrarily well: When $P/T \rightarrow 0$, standard statistical results imply that, under technical conditions, with θ solving (5), $f(x; \theta)$ converges to the ground truth. This simple observation can be formalized as follows: *with enough data, the choice of the function family $f(x; \theta)$ is irrelevant; any family with the universal approximation property will do the job.*

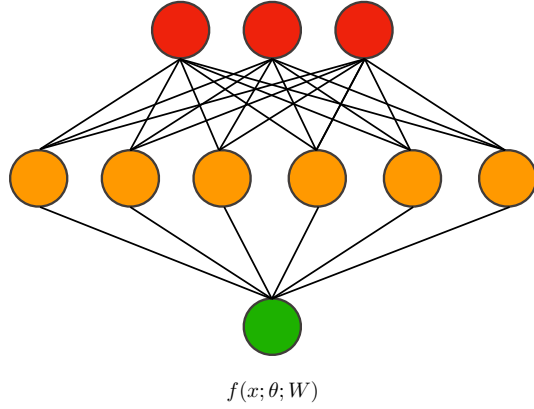
In reality, however, the dimension P of the parameter θ needed to approximate the ground truth efficiently can be very large, typically much larger than T . In this case, any finite sample inference is bound to learn a highly inefficient approximation to $\pi(X)$ due to the *limits to learning*. That is the inability of the estimator to approximate truth when $P/T > 0$. The quality of the learned approximation depends in a subtle way on the complexity $c = P/T$ and the properties of the family $f(x; \theta)$. See, (Didisheim et al., 2023). Thus, *in finite samples, the nature of the function family matters*. And not only that. When θ is high dimensional, finding the *argmin* in (5) becomes an infeasible task. The only thing we can hope for is to come up with an algorithm that somehow finds some meaningful local minimum in (5). Recent discoveries in ML suggest that the nature of this algorithm is also crucial for the behavior of the DNN out-of-sample. See, e.g., (Zhou et al., 2023). That is, *the way we solve (5) for θ matters*. Formally, the tremendous success of Deep Learning is based on the observation that the particular class of parametric families known as DNNs, combined with a particular class of learning algorithms (based on gradient descent), have a powerful ability to approximate truth in the regime where $P > T$, despite insufficient amounts of data. See, e.g., (Nakkiran et al., 2021), (Belkin, 2021). If we want to use deep learning in asset pricing, we need a profound understanding of what and how these models learn about the SDF. Below, we shed some light on this question.

3.1 Factors, Random Features, and Large Factor Models

Before we analyze complex, non-linear function families such as DNNs, it is instructive to consider simpler families that depend linearly on the parameter vector $\theta \in \mathbb{R}^P$. Following (Didisheim et al., 2023), we consider a family

$$f(x; \theta) = f(x; \theta; W) = \sum_{k=1}^P \phi(x'W_k)\theta_k, \quad (6)$$

where $x \in \mathbb{R}^d$ is the input vector of *raw characteristics* and $W_k \in \mathbb{R}^d$ are *random weights*, while $\phi(x)$ is a non-linear *activation function*. The non-linear functions $\phi(x'W_k)$ are known as *random features*. As (Didisheim et al., 2023) explain, a random feature model (6) is



$$\begin{aligned}
 & x \in \mathbb{R}^d \\
 W &= \begin{bmatrix} | & \dots & | & \dots & | \\ W_1 & & W_k & & W_P \\ | & \dots & | & \dots & | \end{bmatrix}_{d \times P} \\
 & \phi(x'W) \\
 & \theta \in \mathbb{R}^P \\
 f(x; \theta) &= f(x; \theta; W) = \sum_{k=1}^P \phi(x'W_k)\theta_k
 \end{aligned}$$

Figure 1: The figure above shows $f(x; \theta; W)$, a mathematical representation of a neural network with a single hidden layer neural network, also known as a shallow network. The weights $W \in \mathbb{R}^{d \times P}$ and $\theta \in \mathbb{R}^P$ are randomly initialized. $\phi : \mathbb{R} \rightarrow \mathbb{R}$ is an elementwise non-linear activation function and the vector $\phi(x'W)$ is also known as *random features*.

equivalent to a *shallow, one hidden layer neural network*, with θ_k being the weights of the output layer, where the weights W_k of the hidden layer are untrained (that is, they are kept constant and are not optimized upon). See, Figure 1.

The linearity of the function family (6) implies that the optimization problem (5) admits a unique, closed-form solution that can be expressed in terms of characteristics-managed portfolios (factors). Namely, defining the vector of factor returns $F_{t+1} = (F_{k,t+1})_{k=1}^P$ with

$$F_{k,t+1} = \sum_{i=1}^{N_t} \underbrace{\phi(X'_{i,t} W_k)}_{k\text{-th random feature}} R_{i,t+1}, \quad (7)$$

we can rewrite the SDF as a factor portfolio,

$$\sum_{i=1}^{N_t} f(X_{i,t}; \theta) R_{i,t+1} = \theta' F_{t+1}. \quad (8)$$

Substituting (8) into (5), we get

$$\theta = \left(zI + T^{-1} \sum_{t=1}^T F_t F_t' \right)^{-1} T^{-1} \sum_{t=1}^T F_t. \quad (9)$$

Thus, the SDF admits an intuitive interpretation for a linear family (6): It is the efficient portfolio of factors.

While conventional logic based on the Arbitrage Pricing Theory (APT) of (Ross, 1976) suggests that the number of factors defining the SDF should be relatively small, (Didisheim et al., 2023) show (both theoretically and empirically) that this intuition breaks down in the world of ML-based factors. Namely, (Didisheim et al., 2023) establish the *virtue of complexity*: The out-of-sample (OOS) performance of the SDF is monotone increasing in the number P of factors, even in the limit of an infinite P . This naturally raises the question: Where does the estimated SDF converge as $P \rightarrow \infty$? To answer this question, we need to introduce some notions from the theory of kernels.

A positive definite kernel on \mathbb{R}^D is a function $K(x, \tilde{x}) : \mathbb{R}^D \times \mathbb{R}^D \rightarrow \mathbb{R}$ such that, for any n vectors $x_i \in \mathbb{R}^D, i = 1, \dots, n$, and any vector $\alpha \in \mathbb{R}^n$, we have

$$\sum_{i_1=1}^n \sum_{i_2=1}^n \alpha_{i_1} \alpha_{i_2} K(x_{i_1}, x_{i_2}) \geq 0. \quad (10)$$

That is, the kernel matrix $\tilde{K} = (K(x_{i_1}, x_{i_2}))_{i_1, i_2=1}^n$ is positive semi-definite. Given some non-linear functions $\phi_k(x), k = 1, \dots, P$ (known as features in ML), we can define a kernel

$$K(x, \tilde{x}) = \frac{1}{P} \sum_{k=1}^P \phi_k(x) \phi_k(\tilde{x}). \quad (11)$$

By direct calculation, K is always positive semi-definite.⁹ The converse is also true: Any positive definite kernel can be approximated by some (potentially highly complex) non-linear features ϕ_k . Formally, by the Mercer theorem (see, e.g., (Bartlett, 2003), (Rahimi and Recht, 2007)), any positive definite kernel $K(x, \tilde{x})$ admits a representation

$$K(x, \tilde{x}) = \int \phi(x; \omega) \phi(\tilde{x}; \omega) p(d\omega), \quad (12)$$

where $p(d\omega)$ is some probability distribution. Hence, sampling W_k from $p(d\omega)$, we can build

⁹Indeed, $\sum_{i_1=1}^n \sum_{i_2=1}^n \alpha_{i_1} \alpha_{i_2} K(x_{i_1}, x_{i_2}) = \frac{1}{P} \sum_k (\sum_i \phi_k(x_i) \alpha_i)^2 \geq 0$.

a Monte-Carlo approximation

$$K(x, \tilde{x}) = \lim_{P \rightarrow \infty} \frac{1}{P} \sum_{k=1}^P \phi(x; W_k) \phi(\tilde{x}; W_k). \quad (13)$$

This representation naturally suggests that in the limit as $P \rightarrow \infty$, the SDF based on the optimal θ from (9) should have a well-defined limit, depending only on the kernel K . In order to compute this limit, we will need a definition.

Definition 1 (The Portfolio Kernel) *Let*

$$Y_t = (R_{t+1}, X_t) \in \mathbb{R}^{N_t(d+1)} \quad (14)$$

be the market state, encompassing all stock characteristics and all stock returns. Given any two market states $Y = (R, X)$, $\tilde{Y} = (\tilde{R}, \tilde{X})$, with $R \in \mathbb{R}^N$, $\tilde{R} \in \mathbb{R}^{\tilde{N}}$, we let

$$K(X, \tilde{X}) = (K(X_i, \tilde{X}_j)) \in \mathbb{R}^{N \times \tilde{N}}, \quad (15)$$

and then define the Portfolio Kernel via

$$\mathbb{K}(Y; \tilde{Y}) = \underbrace{R'}_{1 \times N} K(X, \tilde{X}) \underbrace{\tilde{R}}_{\tilde{N} \times 1}. \quad (16)$$

The Portfolio Kernel operates in the space of market states. For any two such states, it computes a kernel-based similarity measure, $\mathbb{K}(Y; \tilde{Y})$. An extremely useful property of this similarity measure is that it is also a portfolio return: It weights returns R comparing them with returns \tilde{R} in some other market state (e.g., from previous time periods).

We will use

$$Y_{IS} = (R_{t+1}, X_t)_{t=1}^T \in \mathbb{R}^{T \times N_t(d+1)}, \quad (17)$$

to denote the in-sample (IS) data describing the dynamics of the stock market state, Y_t . We also use

$$\bar{\mathbb{K}}_{IS} = (\mathbb{K}(Y_{t_1}; Y_{t_2}))_{t_1, t_2=1}^T \in \mathbb{R}^{T \times T} \quad (18)$$

to denote the *in-sample kernel matrix*, measuring the similarity between in-sample observations.

Let K be a positive definite kernel admitting a representation (12). Let $\{W_k\}_{k=1}^P$ be

independently sampled from $p(d\omega)$, $\phi(x; W_k)$ the corresponding random features, and $F_{t+1} = (F_{k,t+1})_{k=1}^P$

$$F_{k,t+1} = \frac{1}{P^{1/2}} \sum_{i=1}^{N_t} \phi(X_{i,t}; W_k) R_{i,t+1} \quad (19)$$

the corresponding factors. Or, in vector form,

$$F_{t+1} = \frac{1}{P^{1/2}} \phi(X_t; W) R_{t+1} \in \mathbb{R}^P. \quad (20)$$

Let also

$$\theta(z) = \left(zI + T^{-1} \sum_{t=1}^T F_t F_t' \right)^{-1} T^{-1} \sum_{t=1}^T F_t, \quad (21)$$

be the ridge-penalized efficient factor portfolio and $\theta' F_{t+1}$ the corresponding SDF. By direct calculation,

$$\begin{aligned} F_{t+1}' F_{\tau+1} &= \frac{1}{P} R_{t+1}' \phi(X_t; W) \phi(X_\tau; W)' R_{\tau+1} \\ &= R_{t+1}' \left(\frac{1}{P} \sum_{k=1}^P \phi(X_t; W) \phi(X_\tau; W)' \right) R_{\tau+1} \\ &\xrightarrow{(13)} \underbrace{R_{t+1}' K(X_t, X_\tau) R_{\tau+1}}_{(13)} = \mathbb{K}(Y_t, Y_\tau). \end{aligned} \quad (22)$$

That is, the kernel $\mathbb{K}(Y_t, Y_\tau)$ describes the similarity (alignment) between factors at times t, τ . Denoting by $F = (F_t)_{t=1}^T \in \mathbb{R}^{P \times T}$ the in-sample factor returns, we get

$$F' F = (F_{t_1}' F_{t_2})_{t_1, t_2=1}^T \approx (\mathbb{K}(Y_{t_1}, Y_{t_2}))_{t_1, t_2=1}^T = \bar{\mathbb{K}}_{IS}. \quad (23)$$

That is, the matrix $\bar{\mathbb{K}}_{IS}$ measures the similarity between market states by computing the similarity between vectors of factor returns. We will need the following technical lemma.

Lemma 1 *Denote $F \in \mathbb{R}^{P \times T}$ a matrix of in-sample factor returns. Let also $\mathbf{1} = (1, \dots, 1) \in \mathbb{R}^T$ be the vector of ones. Then,*

$$\theta = T^{-1} (zI + T^{-1} F F')^{-1} F \mathbf{1} = T^{-1} F (zI + T^{-1} F' F)^{-1} \mathbf{1}. \quad (24)$$

Lemma 1 is a direct consequence of the regression objective (5): θ is the coefficient

vector from regressing $\mathbf{1} = (1, \dots, 1)$ on factor returns. As a result, by (22),

$$F'_{T+1}\theta = T^{-1} \underbrace{F'_{T+1}F}_{\rightarrow \mathbb{K}(Y_{T+1}, Y_{IS}) \text{ by (22)}} (zI + T^{-1} \underbrace{F'F}_{\rightarrow \bar{\mathbb{K}}_{IS} \text{ by (23)}})^{-1}\mathbf{1}, \quad (25)$$

and we arrive at the following theorem.

Theorem 1 (LFM-SDF) *The Large Factor Model (LFM) SDF is given by*

$$\lim_{P \rightarrow \infty} \theta' F_{T+1} = \mathbb{K}(Y_{T+1}, Y_{IS})\xi = \sum_{t=1}^T \underbrace{\mathbb{K}(Y_{T+1}, Y_t)}_{\text{attention to } t} \underbrace{\xi_t}_{\text{optimal weight}}, \quad (26)$$

where the optimal weights $\xi = (\xi_t)_{t=1}^T$ are given by

$$\xi = \frac{1}{T}(zI + T^{-1}\bar{\mathbb{K}}_{IS})^{-1}\mathbf{1}. \quad (27)$$

Theorem 1 characterizes the limit of the random-feature-based large factor model studied in (Didisheim et al., 2023) as the number of random features grows indefinitely. The LFM-SDF has a very intuitive structure. It uses the Portfolio kernel \mathbb{K} to compare the current state of the whole stock market, as captured by the high-dimensional vector Y_{T+1} , with all past state realizations Y_t , $t = 1, \dots, T$, and pays attention to Y_t depending on their similarity, as captured by the kernel $\mathbb{K}(Y_{T+1}, Y_t)$. This similarity is weighted in a mean-variance efficient manner, determined by the optimal weight vector $\xi \in \mathbb{R}^T$, defining the *optimal time-fixed effects*; i.e., how much each period matters. Naturally, the LFM-SDF also admits a parametric portfolio representation (8), described in the following corollary.

Corollary 2 *We have*

$$\lim_{P \rightarrow \infty} \theta' F_{T+1} = R'_{T+1} f^{\mathbb{K}}(X_t), \quad (28)$$

where

$$f^{\mathbb{K}}(x) = \sum_{t=1}^T \left(\sum_{j=1}^{N_t} R_{j,t+1} K(x, X_{j,t}) \right) \xi_t \quad (29)$$

Thus, the LFM-SDF is, in fact, a characteristics-based factor, based on the single characteristic $f^{\mathbb{K}}(X_{i,t})$.

The elegant representation of the optimal portfolio weight function $f^{\mathbb{K}}(x)$ reveals how the LFM learns from the joint dependency structure between stock returns and their char-

acteristics. For each out-of-sample observation x of characteristics, it compares it with past characteristics of all stocks through the similarity measure $K(x, X_{j,t})$ and weights by stock returns to determine average similarity-weighted performance,

$$Perf_t(x) = \sum_{j=1}^{N_t} R_{j,t+1} K(x, X_{j,t}). \quad (30)$$

It then weights each performance observation $Perf_t(x)$ using the vector ξ , ending up with the optimal function

$$f^K(x) = \sum_{t=1}^T Perf_t(x) \xi_t. \quad (31)$$

To summarize, the analysis of this section shows how, once equipped with a kernel K , we can build an explicit, closed-form SDF that aggregates an infinite number of factors in an (in-sample) efficient way, according to (9). Hence the name ‘‘Large Factor Model’’. This raises two questions. First, how do we select the kernel K ? And second, what does this have to do with deep learning? Below, we provide partial answers to these questions. First, we show that when the neural network is sufficiently wide, the corresponding SDF is, in fact, an LFM for a particular NN-dependent kernel. Second, the in-sample performance of these factors can be used to predict out-of-sample performance and limits-to-learning (Didisheim et al., 2023; Kelly et al., 2023b) and, hence, perform the NN architecture selection based on the corresponding kernel.

4 (Deep) Neural Networks, Gradient Descent, and the Neural Tangent Kernel

We start this section by defining a standard NN architecture, the Multi-Layer Perceptron (MLP). Our results can be extended to other neural architectures based on the results from (Arora et al., 2019; Yang, 2020).

Definition 2 (Multi-Layer Perceptron (MLP)) *Fix a neural network architecture given by the widths of hidden layers (n_1, \dots, n_L) . Let $\theta = (W^0, b^0, \dots, W^{(l)}, b^{(l)})$ be a collection of weights and biases. Here, $W^{(l)} \in \mathbb{R}^{n_l \times n_{l+1}}$, $b^{(l)} \in \mathbb{R}^{n_{l+1}}$, and the total dimension of θ is $P = \sum_{l=1}^{(l)} (n_{l-1} + 1)n_l + n_L$. Let also $\phi : \mathbb{R} \rightarrow \mathbb{R}$ be a Lipschitz, twice differentiable nonlinearity with a bounded second derivative. The MLP neural network $f(x; \theta)$ is defined*

as

$$\begin{aligned}
 x &= \text{input} \in \mathbb{R}^d \\
 y^{(l)}(x) &= \begin{cases} x & \text{if } l = 0, \\ \phi(z^{(l-1)}(x)) & \text{if } l > 0. \end{cases} \\
 z_i^{(l)}(x) &= \frac{1}{n_l^{1/2}} \sum_j W_{ij}^{(l)} y_j^{(l)}(x) + b_i^{(l)},
 \end{aligned} \tag{32}$$

where $y^{(l)}(x), z^{(l-1)}(x) \in \mathbb{R}^{n^{(l)} \times 1}$. The output of the network is

$$f(x; \theta) = z^{(L)}(x) = \frac{1}{n_L^{1/2}} \sum_{j=1}^{n_L} W_j^{(L)} y_j^{(L)}(x). \tag{33}$$

At initialization, all weights $W_{i,j}^{(\ell)}$ and biases $b^{(l)}$ in each hidden layer are sampled independently from $N(0, (\sigma_W^{(l)})^2)$ and $N(0, (\sigma_b^{(l)})^2)$, respectively, for some layer-specific parameters $\sigma_W^{(l)}, \sigma_b^{(l)}$.

Note that we include the weight initialization in the architectural choice. While this initialization is usually ignored in NN analysis (by default, $\sigma_W = \sigma_b = 1$), it plays a crucial role in the behavior of NNs, as shown below.

As a benchmark example, consider a single-hidden-layer NN

$$\begin{aligned}
 f(x; \theta) &= z^1(x) = \frac{1}{n_1^{1/2}} \sum_{k=1}^{n_1} W_k^1 \phi \left(\frac{1}{n_0^{1/2}} \sum_{i=1}^d W_{k,i}^0 x_i + b_k^0 \right) \\
 &= \frac{1}{n_1^{1/2}} \sum_{k=1}^{n_1} W_k^1 \phi \left(\frac{1}{n_0^{1/2}} (W_k^0)' x + b_k^0 \right) \\
 &= \frac{1}{n_1^{1/2}} (W^1)' \phi \left(\frac{1}{n_0^{1/2}} (W^0)' x + b^0 \right).
 \end{aligned} \tag{34}$$

The simple random feature model (6) of (Didisheim et al., 2023) is equivalent to the shallow (single hidden layer) neural network (34), with $\theta = W^1 \in \mathbb{R}^P$, $W_k = W_k^0 \in \mathbb{R}^d$, $P = n_1$. However, there is one important caveat. While (Didisheim et al., 2023) only optimize (train) the output neuron weights W_j^1 (and get (9) for $\theta = W^1$) and keep the random features $W_k = W_k^0$ fixed (untrained), real-world neural networks are trained end-to-end; that is every single weight, including all weights of all hidden layers, is optimized. E.g., for the simple 1-hidden layer net (34), the whole $\theta = (W^1, W^0, b^0) \in \mathbb{R}^{n_1(d+2)}$ is optimized upon. This is

obviously a very hard problem: Plugging $f(x; \theta)$ into (5) leads to a loss function

$$L(\theta) = \frac{1}{T} \sum_{t=1}^T (1 - f(X_t; \theta)' R_{t+1})^2 \quad (35)$$

that is extremely non-convex, with many local minima. In the machine learning jargon, the problem has a complex loss landscape. This is a big problem. If there are so many local minima, which one do we pick?

Things get even more messy in the over-parametrized regime when $P = \dim(\theta)$ is larger than T . In this case, the minimum in (5) is often exactly zero and is achieved for a continuum of points (a manifold of dimension $P - T$), called the *interpolating solutions*: They perfectly interpolate the in-sample data, generating portfolio returns with zero in-sample risk, so that

$$f(X_t; \theta)' R_{t+1} = 1 \text{ for all } t = 1, \dots, T. \quad (36)$$

So, how do we find those interpolating solutions? And how do we pick one among a continuum of them? To this end, we need a numerical algorithm to minimize $L(\theta)$. While one might think that the details of such an algorithm are an unnecessary nuance, it turns out that this intuition is wrong. A deep understanding of the algorithm is necessary for pinning down the nature of DNN-based models.

Most optimization algorithms used for DNNs are based on gradient descent. The idea is simple. Given a *learning rate* $\eta > 0$, we can initialize $\theta = \theta(0)$ randomly, and then let the parameter vector $\theta \in \mathbb{R}^P$ evolve along the direction of the gradient of L :

$$\theta(s + ds) = \theta(s) - \eta ds \nabla_{\theta} L(\theta(s)). \quad (37)$$

By the Taylor approximation, assuming η is sufficiently small,

$$\begin{aligned} L(\theta(s + ds)) &\approx L(\theta(s)) + \nabla_{\theta} L(\theta(s))' (\theta(s + ds) - \theta(s)) \\ &= L(\theta(s)) - \eta ds \|\nabla_{\theta} L(\theta(s))\|^2 \\ &< L(\theta(s)). \end{aligned} \quad (38)$$

Thus, each step of the gradient descent makes the loss function smaller. In the limit of a small learning rate, as $ds \rightarrow 0$, we get the *Gradient Flow*

$$\frac{d\theta(s)}{ds} = -\eta \nabla_{\theta} L(\theta(s)). \quad (39)$$

The continuous gradient flow is an approximation of the standard gradient descent used to train real-world NNs where, after many steps (the analog of the $s \rightarrow \infty$ limit), gradient descent converges to a stationary point satisfying $\nabla_{\theta}L(\theta(s)) = 0$. Using the chain rule, we get that the corresponding NN output, $f(x; \theta(s))$, follows a related ODE:

$$\frac{d}{ds}f(x; \theta(s)) = -\eta \nabla_{\theta}f(x; \theta(s))' \nabla_{\theta}L(\theta(s)). \quad (40)$$

In general, the dynamics of the weight vector $\theta(s)$ and the corresponding prediction, $f(x; \theta(s))$ along the gradient descent path is extremely complicated and non-linear; this is the main reason why DNNs are commonly perceived as “black box” learning machines. Not only does the neural architecture influence $\theta(s)$ in an incomprehensible way, but gradient descent also depends on the initialization. For different $\theta(0)$, we may end up with completely different $f(x; \theta(\infty))$ and, hence, with completely different predictions.¹⁰

A striking discovery of (Jacot et al., 2018) is that in the limit when the net becomes infinitely wide, the outcome of the gradient descent, $f(x; \theta(\infty))$, and its dependence on the initialization, $\theta(0)$, can be characterized explicitly for the mean squared error (MSE) objective $L(\theta) = \frac{1}{T} \sum_t (y_t - f(x_t; \theta))^2$, given some in-sample labels y_t .

4.1 NTK in the Infinite Width Limit

The characterization of (Jacot et al., 2018) is in terms of a specific kernel associated with the NN, known as the *Neural Tangent Kernel (NTK)*. NTK admits an explicit feature representation (11), with features given by the gradient $\nabla_{\theta}f(x; \theta)$:

$$K(x, \tilde{x}; \theta) = \nabla_{\theta}f(x; \theta)' \nabla_{\theta}f(\tilde{x}; \theta) = \sum_{k=1}^P \frac{\partial}{\partial \theta_k} f(x; \theta) \frac{\partial}{\partial \theta_k} f(\tilde{x}; \theta). \quad (41)$$

Formally, (41) is a kernel of enormous complexity. First, the number of features P that this kernel utilizes is huge for typical DNNs. Second, the nature of these features is also complex, as they are intertwined between layers in very subtle ways. However, as (Jacot et al., 2018) show, in the limit as the width of each layer increases indefinitely, (41) converges to a finite, well-behaved limit. In order to characterize this limit, we will need to introduce a different auxiliary kernel that will be important for our analysis.¹¹

¹⁰For example, (Kelly et al., 2023a) show that best results for DNN-based return prediction are obtained by averaging about 40 different random initializations of $\theta(0)$. Furthermore, the pairwise correlations between these predictions are essentially zero; thus, the output of the DNN is extremely sensitive to the initial value $\theta(0)$.

¹¹As (Jacot et al., 2018) show, the neural network at initialization converges to a Gaussian process with the covariance kernel $(\sigma_w^{(L)})^2 \Sigma^{(L+1)}(x, \tilde{x})$.

Definition 3 (The Neural Network Gaussian Process (NNGP) Kernel) *We use*

$$\mathcal{N}(z; \mu, \Sigma) \tag{42}$$

to denote the Gaussian density as a function of $z \in \mathbb{R}^m$ with the mean vector $\mu \in \mathbb{R}^m$ and the covariance matrix $\Sigma \in \mathbb{R}^{m \times m}$. Then, we define

$$\Sigma^{(1)}(x, \tilde{x}) = \frac{1}{n_0} x' \tilde{x} \tag{43}$$

and then, recursively,

$$\Sigma^{(l)}(x, \tilde{x}) = \int dz d\tilde{z} \phi(z) \phi(\tilde{z}) \mathcal{N} \left(\begin{pmatrix} z \\ \tilde{z} \end{pmatrix}; \mathbf{0}, (\sigma_w^{(l-1)})^2 \begin{pmatrix} \Sigma^{(l-1)}(x, x) & \Sigma^{(l-1)}(x, \tilde{x}) \\ \Sigma^{(l-1)}(\tilde{x}, x) & \Sigma^{(l-1)}(\tilde{x}, \tilde{x}) \end{pmatrix} + (\sigma_b^{(l-1)})^2 \mathbf{1}_{2 \times 2} \right) \tag{44}$$

for $l > 1$.

The kernel $(\sigma_w^{(L)})^2 \Sigma^{(L+1)}(x, \tilde{x})$ is known as the Neural Network Gaussian Process (NNGP) kernel (Jacot et al., 2018; Novak et al., 2019).¹² Using $\Sigma^{(l)}$, we can now compute the asymptotic NTK.

Definition 4 (The Infinite Width NTK) *Let*

$$\begin{aligned} \widehat{\Sigma}^{(l)}(x, \tilde{x}) &= (\sigma_w^{(l)})^2 \int dz d\tilde{z} \frac{d}{dz} \phi(z) \frac{d}{d\tilde{z}} \phi(\tilde{z}) \mathcal{N} \left(\begin{pmatrix} z \\ \tilde{z} \end{pmatrix}; \mathbf{0}, (\sigma_w^{(l-1)})^2 \begin{pmatrix} \Sigma^{(l-1)}(x, x) & \Sigma^{(l-1)}(x, \tilde{x}) \\ \Sigma^{(l-1)}(\tilde{x}, x) & \Sigma^{(l-1)}(\tilde{x}, \tilde{x}) \end{pmatrix} + (\sigma_b^{(l-1)})^2 \mathbf{1}_{2 \times 2} \right). \end{aligned} \tag{45}$$

Let also

$$\Theta^{(1)}(x, \tilde{x}) = \Sigma^{(1)}(x, \tilde{x}) + 1, \tag{46}$$

and then define recursively for $l > 1$:

$$\Theta^{(l)}(x, \tilde{x}) = \Theta^{(l-1)}(x, \tilde{x}) \widehat{\Sigma}^{(l)}(x, \tilde{x}) + \Sigma^{(l)}(x, \tilde{x}) + 1 \tag{47}$$

We can now state the result of (Jacot et al., 2018).

¹²The name originates from the fact that the infinitely wide DNN is actually a Gaussian process with NNGP as its covariance kernel.

Theorem 3 (NTK is constant through training for wide NNs (Jacot et al., 2018))

Let $\theta(s)$ follow the gradient descent (37). In the limit as $n_1, \dots, n_L \rightarrow \infty$, the NTK $K(x, \tilde{x}; \theta(s))$ converges to $\Theta^{(L+1)}(x, \tilde{x})$ in probability, uniformly over s in a bounded interval $[0, T]$.

Theorem 3 implies that, in the infinite width limit, the NTK can be expressed through a few simple algebraic manipulations, including an integral over a 2-dimensional Gaussian vector $\begin{pmatrix} z \\ \tilde{z} \end{pmatrix}$ of the product $\phi(z)$ and $\phi(\tilde{z})$.¹³

As an illustration, consider a one-hidden-layer neural network (34). In this case, $\nabla f(x; \theta)$ has three components: The derivative with respect to the hidden layer weights and biases and the derivative with respect to the output layer weights. Denote by

$$z_k(x) = \frac{1}{n_0^{1/2}}(W_k^0)'x + b_k^0, \quad z(x) = (z_k(x))_{k=1}^{n_1} = \frac{1}{n_0^{1/2}}(W^0)'x + b^0 \quad (48)$$

the *pre-activations* of the hidden layer, that serve as inputs to the activation function $\phi(z)$. Note that, conditional on x , $z_k(x)$ are random, dependent on the initialization of the weights. Then,

$$\begin{aligned} & \nabla_{\theta} f(x; \theta) \\ &= \nabla_{\theta} \left(\frac{1}{n_1^{1/2}}(W^1)' \phi \left(\frac{1}{n_0^{1/2}}(W^0)'x + b^0 \right) \right) \\ &= \begin{pmatrix} \nabla_{W^1} f \\ \nabla_{W^0} f \\ \nabla_{b^0} f \end{pmatrix} = \frac{1}{n_1^{1/2}} \begin{pmatrix} \phi(z(x)) \\ W^1 \circ \frac{1}{n_0^{1/2}} \frac{d}{dz} \phi(z(x)) x' \\ W^1 \circ \frac{d}{dz} \phi(z(x)), \end{pmatrix} \end{aligned} \quad (49)$$

where \circ denotes the Kronecker (elementwise) product of matrices. Thus, the NTK (41)

¹³In many practical applications, this integral can be evaluated analytically. For example, this is the case when $\phi(\cdot)$ is given by one of the following activation functions: $ReLU(x) = \max(x, 0)$; $LReLU(x) = x \mathbf{1}_{x>0} + \alpha x \mathbf{1}_{x<0}$; $GELU(x) = x \cdot \Phi(x)$, where $\Phi(x)$ is the cumulative distribution function of a standard normal distribution.

admits the following decomposition

$$\begin{aligned}
\nabla_{\theta} f(x; \theta)' \nabla_{\theta} f(\tilde{x}; \theta) &= \underbrace{K_1(x, \tilde{x})}_{\text{output layer features}} + \underbrace{K_2(x, \tilde{x})}_{\text{hidden layer features}} \\
K_1(x, \tilde{x}) &= \frac{1}{n_1} \sum_{k=1}^{n_1} \phi(z_k(x)) \phi(z_k(\tilde{x})) \\
K_2(x, \tilde{x}) &= \frac{1}{n_1} \sum_{k=1}^{n_1} \left(\frac{1}{n_0} \sum_{i=1}^{n_0} x_i \tilde{x}_i + 1 \right) (W_k^1)^2 \frac{d}{dz} \phi(z_k(x)) \frac{d}{dz} \phi(z_k(\tilde{x})) .
\end{aligned} \tag{50}$$

All three kernel components are random and depend on the weights θ in a highly non-linear fashion. Yet, in the limit as $n_1 \rightarrow \infty$ (i.e., when the single hidden layer becomes infinitely wide), they converge to a deterministic limit by the law of large numbers: We have

$$\begin{pmatrix} z \\ \tilde{z} \end{pmatrix} = \begin{pmatrix} z_k(x) \\ z_k(\tilde{x}) \end{pmatrix} \sim N \left(0, (\sigma_w^0)^2 \begin{pmatrix} \Sigma^{(1)}(x, x) & \Sigma^{(1)}(x, \tilde{x}) \\ \Sigma^{(1)}(\tilde{x}, x) & \Sigma^{(1)}(\tilde{x}, \tilde{x}) \end{pmatrix} + (\sigma_b^0)^2 \mathbf{1} \right)$$

and

$$\begin{aligned}
K_1(x, \tilde{x}) &\rightarrow \Sigma^{(2)}(x, \tilde{x}) = \underbrace{E[\phi(z)\phi(\tilde{z})]}_{\text{Gaussian Integral (44)}} \\
K_2(x, \tilde{x}) &\rightarrow (\Sigma^{(1)}(x, \tilde{x}) + 1) \widehat{\Sigma}^{(1)}(x, \tilde{x})
\end{aligned} \tag{51}$$

where

$$\begin{aligned}
\Sigma^{(1)}(x, \tilde{x}) &= \frac{1}{n_0} x' \tilde{x} \\
\widehat{\Sigma}^{(1)}(x, \tilde{x}) &= \underbrace{(\sigma_w^1)^2 E\left[\frac{d}{dz} \phi(z) \frac{d}{d\tilde{z}} \phi(\tilde{z})\right]}_{\text{Gaussian Integral (45)}} .
\end{aligned} \tag{52}$$

We now discuss the structure of the infinite-width NTK. The gradient with respect to the weights of the output neuron, W^1 , gives the standard random features $\phi(z_k(x))$ used in (6), leading to the $K_1(x, \tilde{x})$ component. By contrast, the $K_2(x, \tilde{x})$ component emerges from the gradient features originating from the gradient descent optimizing over the hidden layer weights, W^0 , b^0 . The corresponding asymptotic kernel thus takes the form

$$\Theta^{(2)} = \underbrace{\Sigma^{(2)}(x, \tilde{x})}_{\text{random features (6)}} + \underbrace{(\Sigma^{(1)}(x, \tilde{x}) + 1) \widehat{\Sigma}^{(1)}(x, \tilde{x})}_{\text{training hidden weights}} . \tag{53}$$

The next section uses the (infinite-width) NTK to describe the DNN-SDFs. In the SDF

setting, the two components correspond to different factors based on the characteristics (gradient features) described above.

4.2 The Portfolio Tangent Kernel and the DNN-SDF

Our goal is to understand the behavior of the DNN $f(x; \theta)$ trained by gradient descent to minimize the objective (5) with $z = 0$. Introducing the characteristics-based factor return function

$$F(R, X; \theta) = R' f(X; \theta), \quad (54)$$

we can rewrite the objective as

$$\min_{\theta} \frac{1}{T} \sum_{t=1}^T (1 - F(R_{t+1}, X_t; \theta))^2.$$

The gradient descent is thus forced to move $\theta(s)$ along the directions that make $F(R, X; \theta)$ as close as possible to 1 on the training (i.e., in-sample) data and the dynamics of $\theta(s)$ along the gradient descent path are determined by the properties of $\nabla_{\theta} F(R, X; \theta) = R' \nabla_{\theta} f(X; \theta)$. That is, the gradient of the characteristics-based factor return is itself a vector of characteristics-based factor returns, with characteristics given by the gradient features, $\nabla_{\theta} f(X; \theta)$. We can now introduce the following definition.

Definition 5 (The Portfolio Tangent Kernel (PTK)) *Let $R \in \mathbb{R}^N$, $\tilde{R} \in \mathbb{R}^{\tilde{N}}$, and define*

$$\mathbb{K}((R, X); (\tilde{R}, \tilde{X}); \theta) = \underbrace{R'}_{1 \times N} \underbrace{\nabla_{\theta} f(X; \theta)}_{N \times P} \underbrace{\nabla_{\theta} f(\tilde{X}; \theta)'}_{P \times \tilde{N}} \underbrace{\tilde{R}}_{\tilde{N} \times 1}. \quad (55)$$

to be the tangent kernel for the function $F(R, X; \theta)$. We refer to it as the Portfolio Tangent Kernel (PTK).

Clearly, PTK is a Portfolio Kernel of Definition 1, with the kernel K being the Tangent Kernel for the parametric family $f(X; \theta)$: By (41),

$$\mathbb{K}((R, X); (\tilde{R}, \tilde{X}); \theta) = R' K(X, \tilde{X}; \theta) \tilde{R}. \quad (56)$$

When θ is high-dimensional, \mathbb{K} exhibits an enormous complexity, aggregating a huge number of characteristics-based factors

$$F_{k,t+1} = R'_{t+1} \nabla_{\theta_k} f(X_t; \theta), \quad k = 1, \dots, P. \quad (57)$$

Namely, for any two time instants t, τ , we have

$$\begin{aligned} \mathbb{K}(Y_t; Y_\tau) &= \mathbb{K}((R_{t+1}, X_t); (R_{\tau+1}, X_\tau); \theta) \\ &= R'_{t+1} \nabla_{\theta} f(X_t; \theta) \nabla_{\theta} f(X_\tau; \theta)' R_{\tau+1} \\ &= R'_{t+1} \sum_k \nabla_{\theta_k} f(X_t; \theta) \nabla_{\theta_k} f(X_\tau; \theta) R_{\tau+1} \\ &= \sum_{k=1}^P \underbrace{R'_{t+1} \nabla_{\theta_k} f(X_t; \theta)}_{F_{k,t+1}} \underbrace{\nabla_{\theta_k} f(X_\tau; \theta) R_{\tau+1}}_{F_{k,\tau+1}} \\ &= \sum_{k=1}^P F_{k,t+1} F_{k,\tau+1} = F'_{t+1} F_{\tau+1}. \end{aligned} \quad (58)$$

That is, $\mathbb{K}(Y_t, Y_\tau)$ is a similarity measure of factor returns, comparing how factor return vectors $F_{t+1} \in \mathbb{R}^P$ and $F_{\tau+1} \in \mathbb{R}^P$ are aligned across time periods.

With this interpretation of the PTK at our disposal, we can now proceed to understand how PTK behaves in the infinite-width limit. By Theorem 3, when $P \rightarrow \infty$, in the limit as $P \rightarrow \infty$, $K(X, \tilde{X}; \theta) \rightarrow \Theta^{(L+1)}(X, \tilde{X})$ and, hence, we get¹⁴

Corollary 4 (Infinite Width PTK) *Under the hypothesis of Theorem 3, the infinite-width PTK is independent of θ :*

$$\mathbb{K}((R, X); (\tilde{R}, \tilde{X}); \theta) \rightarrow \mathbb{K}^\infty((R, X); (\tilde{R}, \tilde{X})) = R' \Theta^{(L+1)}(X, \tilde{X}) \tilde{R}. \quad (59)$$

We refer to \mathbb{K}^∞ as the infinite width PTK. As in (18), we use

$$\bar{\mathbb{K}}_{IS}^\infty = (\mathbb{K}^\infty(Y_{t_1}; Y_{t_2}))_{t_1, t_2=1}^T \in \mathbb{R}^{T \times T} \quad (60)$$

to denote the kernel-based similarity matrix of all past states of the economy, based on the PTK \mathbb{K}^∞ . Our goal is to derive an explicit, analytical expression for the DNN-SDF after s steps of gradient descent (see (40)),

$$F(R, X; \theta(s)) = R' f(X; \theta(s)) \quad (61)$$

¹⁴See, also, (Arora et al., 2019; Yang and Hu, 2021).

in the infinite width limit as $n_1, \dots, n_L \rightarrow \infty$. Recall that $Y = (R, X)$ is the state of the stock market and $Y_{IS} = (Y_t)_{t=1}^T$, $Y_t = (R_{t+1}, X_t)$ is the in-sample data. The following is true.

Theorem 5 (Closed-Form Wide DNN-SDFs) *Under the hypothesis of Theorem 3, we have*

$$F(Y; \theta(s)) \approx F(Y; \theta(0)) + \frac{1}{T} \mathbb{K}^\infty(Y, Y_{IS}) \xi(s, \theta(0)), \quad (62)$$

where

$$\xi(s, \theta(0)) = \left(\frac{1}{T} \bar{\mathbb{K}}_{IS}^\infty\right)^{-1} (I - e^{-\frac{1}{T} \bar{\mathbb{K}}_{IS}^\infty s}) (\mathbf{1} - F(Y_{IS}; \theta(0))) \quad (63)$$

When averaged over a large number m of random initializations $\theta_i(0), i = 1, \dots, m$, this expression converges to

$$\bar{F}(Y; s) = \frac{1}{m} \sum_{i=1}^m F(Y; \theta_i(s)) \xrightarrow{m \rightarrow \infty} \frac{1}{T} \mathbb{K}^\infty(Y, Y_{IS}) \bar{\xi}(s), \quad (64)$$

where

$$\bar{\xi}(s) = \left(\frac{1}{T} \bar{\mathbb{K}}_{IS}^\infty\right)^{-1} (I - e^{-\frac{1}{T} \eta \bar{\mathbb{K}}_{IS}^\infty s}) \mathbf{1}. \quad (65)$$

Theorem 5 offers a major insight into the nature of Wide DNN-SDF. First, it makes the dependence on the initialization completely explicit: Each random seed used to generate a different initial weight vector $\theta(0)$ will lead to a different prediction contaminated by noise. This noise contaminates the function both through its initial value, $F(Y; \theta(0))$, and the weight vector, which converges to a different local minimum $\xi(s; \theta(0))$ that depends on $\theta(0)$. Second, it shows explicitly the role of the number of steps of the gradient descent algorithm, as captured by the exponential term, $e^{-\eta \bar{\mathbb{K}}_{IS}^\infty s}$. Thus, the learning rate η acts as a regularizer, akin to the ridge penalty in the ridge regression. To understand the underlying mechanism, let us perform the spectral decomposition $\bar{\mathbb{K}}_{IS}^\infty = UDU'$. Then,

$$\begin{aligned} \left(\frac{1}{T} \bar{\mathbb{K}}_{IS}^\infty\right)^{-1} (I - e^{-\frac{1}{T} \eta \bar{\mathbb{K}}_{IS}^\infty s}) &= U f_{GD}(D) U' \\ (zI + \frac{1}{T} \bar{\mathbb{K}}_{IS}^\infty)^{-1} &= U f_{ridge}(D) U', \end{aligned} \quad (66)$$

where

$$\begin{aligned} f_{GD}(x) &= x^{-1} (1 - e^{-\eta s x}) \\ f_{ridge}(x) &= x^{-1} \frac{1}{1 + x^{-1} z}. \end{aligned} \tag{67}$$

Thus, the DNN-SDF (64) and its ridge-penalized analog (Theorem 1) are given by

$$\begin{aligned} SDF^{Ridge} &= \mathbb{K}(Y_{T+1}, Y_{IS}) \xi_{ridge}(z) \\ SDF^{DNN} &= \mathbb{K}(Y_{T+1}, Y_{IS}) \bar{\xi}(s), \end{aligned} \tag{68}$$

where

$$\begin{aligned} \bar{\xi}(s) &= U(D^{-1}(1 - e^{-\eta s D}))U' \mathbf{1} \\ \xi_{ridge}(z) &= U((z + D)^{-1})U' \mathbf{1}. \end{aligned} \tag{69}$$

Both the gradient descent-based estimator $\bar{\xi}(s)$ (averaged across multiple seeds) and the ridge estimator $\xi_{ridge}(z)$ are spectral shrinkage estimators in the language of (Kelly et al., 2023b): They both shrink the covariance matrix transforming its eigenvalues and punishing smaller eigenvalues more. The fact the gradient descent on DNNs “discovers” spectral shrinkage is striking. It suggests that many standard learning algorithms have hidden, implicit regularization mechanisms that might be responsible for their superior performance. Recent discoveries in the machine learning literature (Zhou et al., 2023) confirm this intuition.

If the kernel matrix \mathbb{K}_{IS}^∞ is strictly positive definite, then, as $s \rightarrow \infty$ (after sufficiently many gradient descent steps), the term $e^{-\eta \bar{\mathbb{K}}_{IS}^\infty s}$ in (65) vanishes, and we recover the standard kernel (ridgeless) regression

$$\lim_{s \rightarrow \infty} \bar{F}(Y; s) \approx \mathbb{K}^\infty(Y, Y_{IS}) (\bar{\mathbb{K}}_{IS}^\infty)^{-1} \mathbf{1}. \tag{70}$$

Thus, we arrive at the following result.

Corollary 6 (Wide DNN-SDFs are LFMs) *In the limit of wide DNNs trained for a sufficiently long time, the DNN-SDF averaged over sufficiently many seeds converges to the LFM-SDF of Theorem 1, with $\mathbb{K} = \mathbb{K}^\infty$. Thus, the DNN-SDF is the in-sample mean-variance efficient portfolio (21) with the factors $F_{t+1} = (F_{k,t+1})_{k=1}^P$ given by*

$$F_{k,t+1} = R'_{t+1} \nabla_{\theta_k} f(X_{i,t}; \theta). \tag{71}$$

Strikingly, Corollary 6 implies that DNN-SDF behaves like a human economist who

believes in factor models. It builds characteristics summarizing the *inductive biases* of the neural net, incorporating its architecture and initialization (the distribution of weights). The formula (47) allows us to derive these characteristics analytically and understand the nature of features that DNN-SDF uses to build factors. Namely, by (47),

$$\mathbb{K}^\infty(x, \tilde{x}) = \Theta^{(L)}(x, \tilde{x})\widehat{\Sigma}^{(L)}(x, \tilde{x}) + \Sigma^{(L)}(x, \tilde{x}) \quad (72)$$

It is possible to show ((Jacot et al., 2018); see Theorem 8 in the Appendix for a proof) that $\Sigma^{(L)}(x, \tilde{x})$ admits an intuitive interpretation: It is the kernel for random features $z^{(L)}(x)$ generated by the last hidden layer of the *untrained neural network* from Definition 2, similarly to the random features (6) for the shallow (one hidden layer) network. At the same time, the product $\Theta^{(L)}(x, \tilde{x})\widehat{\Sigma}^{(L)}(x, \tilde{x})$ is responsible for the optimization (learning) of the hidden layer weights and encompasses random gradient features from all hidden layers. Thus, we obtain the following result.

Corollary 7 (DNN-SDF Subsumes Random Features) *The LFM of Corollary 6 is equivalent to a factor model that contains the n_L factors based on the random features $z^{(L)}(x) = \nabla_{W^{(L)}} f(x; \theta)$, as well as factors originating from the derivatives $\nabla_{\theta_k} f(X_{i,t}; \theta)$ with respect to the parameters of hidden layers.*

Corollary 7 provides an important insight into how DNNs learn. This can already be understood for the single hidden layer case, which we analyze here in detail. From (49)-(50), we get that the LFM underlying a single-hidden layer network is built from three groups of factors:

$$F'_{t+1} = \left(\underbrace{(F_{t+1}^{(1)})'}_{\in \mathbb{R}^{n_1}}, \underbrace{(F_{t+1}^{(2)})'}_{\in \mathbb{R}^{n_1 n_0}}, \underbrace{(F_{t+1}^{(3)})'}_{\in \mathbb{R}^{n_1}} \right), \quad (73)$$

where

$$\begin{aligned} F_{k,t+1}^{(1)} &= \frac{1}{n_1^{1/2}} R'_{t+1} \phi(z_k(X_t)), \quad k = 1, \dots, n_1 \\ F_{k_0, k_1, t+1}^{(2)} &= \frac{1}{n_1^{1/2} n_0^{1/2}} R'_{t+1} (W_{k_1}^1 X_t(k_0) \frac{d}{dz} \phi(z_{k_1}(X_t))), \quad k_0 = 1, \dots, n_0; \quad k_1 = 1, \dots, n_1 \\ F_{k,t+1}^{(3)} &= \frac{1}{n_1^{1/2}} R'_{t+1} W_k^1 \frac{d}{dz} \phi(z_k(X_t)) \end{aligned} \quad (74)$$

This shows how, in addition to the simple random-feature-based factors (6) studied in (Didisheim et al., 2023), the NN “discovers” two other types of random features. The second

group of these features has a huge dimension of $n_0 n_1$: Through these features, the NN tries to figure out the impact of varying the hidden layer weights and biases on the Sharpe ratio of the factor portfolio. As (Adlam and Pennington, 2020) argue, these features have more structure to them than the plain random features of the first group of factors, leading to potentially better out-of-sample performance. The interpretation of DNN-SDF as a factor model based on multiple classes of random features (each class corresponding to a specific group of neural net coefficients in a specific layer) has important implications for the out-of-sample performance of this SDF. As (Didisheim et al., 2023) show, (6) exhibits behavior analogous to that of the classical double descent: The fact that, in regression problems, the OOS error first decreases, then increases, and then decreases again; see, (Belkin et al., 2018; Hastie et al., 2022). The only difference is that (as in (Kelly et al., 2022)), double descent is replaced with double ascent. Namely, the OOS Sharpe ratio first increases and then decreases in $P \in [1, T]$. But then, for $P > T$, in the so-called over-parametrized regime, the Sharpe ratio increases again and flattens out around the complexity level $c = P/T \approx 100$. Furthermore, (Adlam and Pennington, 2020) and (Meng et al., 2022) show that, in the standard regression setting, double descent is replaced with multiple descent when we have multiple groups of random features in the model: The OOS error increases and decreases multiple (more than two) times. We conjecture that DNN-SDFs exhibit multiple ascent phenomena on their path to the infinite width limit studied here. Investigating these phenomena is an important direction for future research.

5 Empirics

Training and testing SDFs based on actual, wide neural networks and large panel datasets requires huge computational resources. When the network is wide enough, it might even become impossible, as one would need to train a network with trillions of parameters. In this section, we leverage the closed-form expression for the infinite-width limit (64) and investigate its ability to generate DNN-SDFs that work out-of-sample. To stay consistent with the analysis in (Didisheim et al., 2023) and the definition of LFMs in Theorem 1, we use ridge regularization instead of the early stopping regularization arising from gradient descent in (64). That is, we investigate the properties of DNN-SDFs given by the explicit formula

$$\bar{F}(Y_{T+1}; z) = \mathbb{K}^\infty(Y_{T+1}, Y_{IS}) (\bar{\mathbb{K}}_{IS}^\infty + z I_{T \times T})^{-1} \mathbf{1}, \quad (75)$$

where z is the ridge penalty.

We consider a grid of ridge penalties $z \in \{10^{-5}, 10^{-4}, 10^{-3}, 10^{-2}, 10^{-1}, 10^0, 10^1, 10^2, 10^3\}$ and use rolling windows of $T = \{12, 60, 120\}$ months. Our key observation is that formula (75) only requires computing the kernel matrix $\mathbb{K}_{IS}^\infty \in \mathbb{R}^{T \times T}$ and the cross-kernel matrix $\mathbb{K}^\infty(Y_{T+1}, Y_{IS}) \in \mathbb{R}^T$ comparing the out-of-sample market state with all in-sample states in the rolling window of length T . Since N_t is large, we need some form of normalization to make the kernel matrix well-behaved. To this end, we normalize

$$\mathbb{K}_{IS}^\infty(t_1, t_2) = R'_{t_1} K(X_{t_1}, X_{t_2}) R_{t_2} \frac{1}{N_{t_1}^\alpha N_{t_2}^\alpha}. \quad (76)$$

Everywhere in the sequel, we use $\alpha = 0.5$.¹⁵ We retrain the model every six months to reduce computing costs. We leverage recent advances in the computation of NTK (see, (Novak et al., 2020); (Novak et al., 2022); (Hron et al., 2020); (Sohl-Dickstein et al., 2020); and (Han et al., 2022)) together with the publicly available package neural tangents.¹⁶ While we cannot avoid computing the full NTK kernel matrix $K(X_{IS}) = (K(X_{i_1, t_1}, X_{i_2, t_2}) : i_k \in \{1, \dots, N_{t_k}\}, t_k = 1, \dots, T, k = 1, 2) \in \mathbb{R}^{(NT) \times (NT)}$ where $N = T^{-1} \sum_t N_t$, we can utilize additivity of the \mathbb{K}_{IS}^∞ matrix and compute $K(X_{IS})$ in chunks. Namely, we use the identity

$$\mathbb{K}_{IS}^\infty(t_1, :) = \frac{1}{N_{t_1}^\alpha} R'_{t_1} K(X_{t_1}, X_{IS}) R_{IS} (N_{t_2}^{-\alpha})_{t_2=1}^T \in \mathbb{R}^T \quad (77)$$

and loop through t_1 , computing each row of \mathbb{K}_{IS} separately. Alternatively, when T is too large so that $K(X_{t_1}, X_{IS}) \in \mathbb{R}^{N_{t_1} \times NT}$ does not fit into RAM, we can utilize a double loop over t_1, t_2 and compute (76) for each t_1, t_2 or for mini-batches of time periods, with the sizes of these mini-batches chosen to optimize the speed-RAM tradeoff.

Our extensive discussion of random features and the link between the NTK and the “naive” model (6) motivates us to study both NTK and its “pure random feature counterpart” $\Sigma^{(L+1)}(x, \tilde{x})$. We thus investigate two separate kernel models:

$$\mathbb{K}^{NTK} = \mathbb{K}^\infty, \mathbb{K}^{NNGP} = (\sigma_w^{(L)})^2 \Sigma^{(L+1)}. \quad (78)$$

By (72), \mathbb{K}^{NNGP} is, in fact, a component of NTK. As we explain above, the NNGP kernel \mathbb{K}^{NNGP} is based on random features given by a randomly initialized NN (Theorem 8 in the Appendix); thus, it is the natural analog of (6) to deeper NNs. Depth is important for both NTK and NNGP. However, there are important differences. NNGP is always built from exactly n_L random features, independent of the depth; only the nature of these features changes with the architecture. By contrast, NTK has an astronomical number

¹⁵We have also produced results for $\alpha = 1$. These results are available upon request.

¹⁶<https://github.com/google/neural-tangents>

$P = \sum_{l=1}^L (n_{l-1} + 1)n_l + n_L$ of features, accounting for numerous subtle non-linearities hidden in the gradient of the DNN. Hence, intuitively, we expect depth to have a stronger effect on NTK than on NNGP. We consider the standard empirical problem of estimating the SDF from US stock returns at a monthly frequency (see (Lettau and Pelger, 2020; Kozak et al., 2020a)). In addition to stock returns, we require data on the conditioning variables, X_t , and use the data set constructed in (Jensen et al., 2023) (JKP henceforth), which is a comprehensive and standardized collection of stock-level return predictors from the finance literature.¹⁷ It includes monthly observations of 153 characteristics for each stock from 1963 to 2022. The JKP universe includes NYSE/AMEX/NASDAQ securities with CRSP share code 10, 11, or 12, excluding “nano” stock as classified by JKP (i.e., stocks with market capitalization below the first percentile of NYSE stocks). Some of the JKP characteristics have low coverage, especially in the early parts of the sample. To ensure that characteristic composition is fairly homogeneous over time and to avoid purging a large number of stock-month observations due to missing data, we reduce the 153 characteristics to a smaller set of 131 characteristics with the fewest missing values. We drop stock-month observations for which more than 1/3 of the 131 characteristic values are missing and use N_t to denote the number of the remaining stock observations at time t . Next, we cross-sectionally rank-standardize each characteristic and map it to the $[-0.5, 0.5]$ interval, following (Gu et al., 2020b). Ultimately, we obtain a panel of characteristics $X_t = (X_{i,k,t})_{i,k} \in \mathbb{R}^{N_t \times d}$, $d = 131$. We use Definition 2 and investigate MLP DNNs in the infinite width limit. By definition, each such infinite width DNN is uniquely pinned down by the choice of L , $\sigma_w^{(l)}$, $\sigma_b^{(l)}$, and the activation function $\phi(x)$. We study a large set of architectures with depth given by a power of two, $L = 1, 2, 4, 8, \dots, 128$. We use the standard weight initialization $\sigma_w^{(l)} = 1$, $\sigma_b^{(l)} = 0.05$ for all l . In the sequel, we refer to this weight initialization as *Flat*. Finally, we consider two different activation functions, $\phi(x) = \text{ReLU}(x) = \max(x, 0)$, and $\phi(x) = \text{Erf}(x)$.¹⁸

We chose these functions because of their highly distinct properties. ReLU is a non-smooth function growing linearly at infinity and, hence, suffering less from the so-called vanishing gradient problem. Erf(x) is a smooth, sigmoid-like function, which is flat for large values of $|x|$. In all of our analysis, in addition to absolute performance measures (such as

¹⁷The JKP stock-level data are accessible at <https://wrds-www.wharton.upenn.edu/pages/get-data/contributed-data-forms/global-factor-data/>.

¹⁸

$$\text{Erf}(x) = \frac{2}{\sqrt{\pi}} \int_0^x e^{-t^2} dt$$

replaces the standard sigmoid $\sigma(x) = e^x / (1 + e^x)$ in the NTK analysis because it allows us to evaluate the Gaussian integrals (44), (45) analytically with $\phi(z) = \text{Erf}(z)$.

the Sharpe Ratio), we also report the t-statistic of alpha from the regression

$$R_{t+1}^{DNN} = \alpha + \beta_1 Mkt_{t+1} + \beta_2 HML_{t+1} + \beta_3 SMB + \beta_4 MOM_{t+1} + \beta_5 STR_{t+1} + \beta_6 LTR_{t+1} + \beta_7 R_{t+1}^{DKKM}. \quad (79)$$

Here, R_{t+1}^{DNN} is computed using formula (75); Market, HML, SMB, Monthly 2-12 Momentum, Short-Term Revert (STR) and Long-Term Reversal (LTR) are from the Kenneth R. French data library. Finally, R_{t+1}^{DKKM} is the best SDF from (Didisheim et al., 2023). The latter factor is particularly important for us: (Didisheim et al., 2023) construct the SDF from a simple, one-hidden-layer neural net with a sin and cos non-linearity; hence, it serves as a natural benchmark for SDFs constructed using more complex neural networks.

We start our discussion with the results for the shortest rolling window of 12 months. In this case, we are effectively estimating our factor similarity matrix (58) based on only 12 observations, implying tremendous complexity and limits to learning in the language of (Didisheim et al., 2023). Figure 2 reports the performance of the DNN-SDF changes as a function of depth, with the standard activation function $\phi(x) = \text{ReLU}(x)$. While we clearly see that depth does add a bit to performance, its gain is small, and the performance quickly saturates around depth = 4, after which adding more hidden layers deteriorates performance, illustrating a form of overfit: The DNN finds spurious patterns that simply cannot be identified with just 12 months of data. As we discussed above, the key difference between DNNs and random feature models comes from the contributions of the hidden layers. To highlight these contributions, we compare the performance of the two kernels (78) in Figure 3. As we can see, for small depth levels, NTK is indeed able to extract valuable information from the hidden layers, but this value vanishes quickly as we make the net deeper because it is diluted across “too many layers of noise”. We observe similar patterns when using $\phi(x) = \text{Erf}(x)$ in Figures 4 and 5. Although with Erf, the alpha of the NNGP-SDF does improve until we reach the depth of 60, this improvement is small. The Sharpe ratio of the DNN-SDF (that is, the NTK-SDF) deteriorates after the depth of 4. One interesting pattern we observe is that the optimal depth is greater for NNGP than for NTK: NNGP, although being based on purely random features, finds it easier to extract information from depth. By contrast, NTK just has too many random features (gradients with respect to all the hidden layers), and it is not able to learn to exploit them efficiently with the little data available.

The results for the rolling window of 60 months for $\phi(x) = \text{ReLU}(x)$ are reported in Figures 6 and 7. Here, with five times more data available to the DNNs, we finally see the emergence of the *virtue of depth complexity*: First, the Sharpe ratio of NTK is monotone,

increasing in depth and saturates only around a depth of 16. Yet, perhaps surprisingly, the t-statistic of alpha in the multi-variate first drops and then starts monotonically increasing, suggesting that DNNs are indeed capturing sources of non-linear alpha that are different from those found in (Didisheim et al., 2023). Figure 7 shows that NTK indeed manages to find alpha not covered by NNGP, and this alpha saturates around the depth of 16, clearly indicating the virtue of using deeper NNs for SDF construction. The results in Figures 8 and 9 and $\phi(x) = \text{Erf}(x)$ covering the case of the *Erf* activation function are relatively similar.

Figures 10 and 11 report the results for the rolling window of 120 months and $\phi(x) = \text{ReLU}(x)$ activation function. As one can see, the shallow, depth-one model and the deep, 128-hidden-layer model have comparable Sharpe Ratios around 3.3. Yet, the deep model has an alpha that is almost double that of the shallow model, clearly indicating that the deep model can identify novel non-linear characteristics not contained in the standard (or shallow) models.

6 Conclusions

Deep learning is revolutionizing the world, affecting almost every aspect of our everyday life. It seems unavoidable that it will profoundly impact finance and economics research in the coming years. For this to happen, we must develop a theoretical understanding of what deep learning actually does for classical economic and statistical problems. In this paper, we take a first step towards understanding the mechanisms behind deep learning applied to the problem of estimating the SDF.

The conventional approach to this estimation problem is based on the idea of factors. Motivated by the APT considerations and the ideas of sparsity, most academic papers attempt to build an SDF as a low-dimensional factor portfolio; these factors are typically constructed based on stock characteristics. The recent results (Didisheim et al., 2023) suggest that such characteristics-based factors span the SDF. However, as both (Didisheim et al., 2023) and (Kozak and Nagel, 2023b) show, we need many characteristics to achieve smaller pricing errors. The virtue of complexity introduced in (Didisheim et al., 2023) suggests that, despite the massive in-sample overfit, it is beneficial to build models with a very large number of factors, and such models perform better out-of-sample. In this paper, we show that DNN-based SDFs do exactly this. Namely, they build an SDF from a very large number of factors. These factors are based on characteristics constructed by the DNN as non-trivial *features* that are potentially useful for cross-sectional asset pricing. The deeper the NN, the more sophisticated features it constructs. We study these features empirically and show

that, indeed, with a sufficient amount of data, deeper nets are able to identify features that improve out-of-sample performance, illustrating *the virtue of depth complexity*.

The analytical tractability of the infinite-width neural nets studied in this paper comes at a cost. While the DNN does generate interesting features, they are entirely random, and the net just constructs a gigantic “kitchen sink” portfolio based on them. In the ML jargon, *no feature learning* happens in our limit because the DNN operates in the *kernel regime*. It is known (Yang and Hu, 2021) that feature learning only occurs in DNNs under specific parametrizations. However, the kernel methods, such as the NTK and NNGP kernels studied in our paper, are no longer useful in describing such DNN models; see, e.g., (Kelly et al., 2023a). Investigating the ability of DNNs to learn features for asset pricing is an important direction for future research.

References

- Adlam, Ben and Jeffrey Pennington**, “The neural tangent kernel in high dimensions: Triple descent and a multi-scale theory of generalization,” in “International Conference on Machine Learning” PMLR 2020, pp. 74–84.
- Andreini, Paolo, Cosimo Izzo, and Giovanni Ricco**, “Deep dynamic factor models,” *arXiv preprint arXiv:2007.11887*, 2020.
- Arora, Sanjeev, Simon S Du, Wei Hu, Zhiyuan Li, Russ R Salakhutdinov, and Ruosong Wang**, “On exact computation with an infinitely wide neural net,” *Advances in neural information processing systems*, 2019, 32.
- Avramov, Doron, Si Cheng, and Lior Metzker**, “Machine learning vs. economic restrictions: Evidence from stock return predictability,” *Management Science*, 2023, 69 (5), 2587–2619.
- Bartlett, Peter**, “Reproducing kernel Hilbert spaces,” *Lecture Notes, CS281B/Stat241B, Statistical Learning Theory*, 2003.
- Belkin, M, D Hsu, S Ma, and S Mandal**, “Reconciling modern machine learning and the bias-variance trade-off. arXiv e-prints,” 2018.
- Belkin, Mikhail**, “Fit without fear: remarkable mathematical phenomena of deep learning through the prism of interpolation,” *Acta Numerica*, 2021, 30, 203–248.
- Britten-Jones, Mark**, “The Sampling Error in Estimates of Mean-Variance Efficient Portfolio Weights,” *Journal of Finance*, 1999, 54 (2), 655–670.
- , “The sampling error in estimates of mean-variance efficient portfolio weights,” *The Journal of Finance*, 1999, 54 (2), 655–671.
- Bryzgalova, Svetlana, Markus Pelger, and Jason Zhu**, “Forest through the trees: Building cross-sections of stock returns,” *Available at SSRN 3493458*, 2020.
- Chen, Luyang, Markus Pelger, and Jason Zhu**, “Deep learning in asset pricing,” *Management Science*, 2023.
- Chinco, Alex, Adam D Clark-Joseph, and Mao Ye**, “Sparse signals in the cross-section of returns,” *The Journal of Finance*, 2019, 74 (1), 449–492.
- Cochrane, John H**, “Presidential address: Discount rates,” *The Journal of finance*, 2011, 66 (4), 1047–1108.
- Didisheim, Antoine, Shikun Ke, Bryan T Kelly, and Semyon Malamud**, “Complexity in Factor Pricing Models,” *Swiss Finance Institute Research Paper*, 2023, (23-19).
- Dixon, Matthew and Nick Polson**, “Deep fundamental factor models,” *SIAM Journal on Financial Mathematics*, 2020, 11 (3), SC26–SC37.

- Fan, Jianqing, Zheng Tracy Ke, Yuan Liao, and Andreas Neuhierl**, “Structural Deep Learning in Conditional Asset Pricing,” *Available at SSRN 4117882*, 2022.
- Feng, Guanhao, Jingyu He, Nicholas G Polson, and Jianeng Xu**, “Deep learning in characteristics-sorted factor models,” *arXiv preprint arXiv:1805.01104*, 2018.
- , **Liang Jiang, Junye Li, and Yizhi Song**, “Deep Tangency Portfolios,” *Available at SSRN 3971274*, 2023.
- , **Stefano Giglio, and Dacheng Xiu**, “Taming the factor zoo: A test of new factors,” *The Journal of Finance*, 2020, *75* (3), 1327–1370.
- Filipović, Damir and Puneet Pasricha**, “Empirical Asset Pricing via Ensemble Gaussian Process Regression,” *arXiv preprint arXiv:2212.01048*, 2022.
- Freyberger, Joachim, Andreas Neuhierl, and Michael Weber**, “Dissecting characteristics nonparametrically,” *The Review of Financial Studies*, 2020, *33* (5), 2326–2377.
- Ghorbani, Behrooz, Song Mei, Theodor Misiakiewicz, and Andrea Montanari**, “When do neural networks outperform kernel methods?,” *Advances in Neural Information Processing Systems*, 2020, *33*, 14820–14830.
- Giglio, Stefano, Bryan Kelly, and Dacheng Xiu**, “Factor models, machine learning, and asset pricing,” *Annual Review of Financial Economics*, 2022, *14*, 337–368.
- Gu, Shihao, Bryan Kelly, and Dacheng Xiu**, “Autoencoder Asset Pricing Models,” *Journal of Econometrics*, 2020.
- , —, and —, “Empirical asset pricing via machine learning,” *The Review of Financial Studies*, 2020, *33* (5), 2223–2273.
- Guijarro-Ordóñez, Jorge, Markus Pelger, and Greg Zanolli**, “Deep learning statistical arbitrage,” *arXiv preprint arXiv:2106.04028*, 2021.
- Han, Insu, Amir Zandieh, Jaehoon Lee, Roman Novak, Lechao Xiao, and Amin Karbasi**, “Fast Neural Kernel Embeddings for General Activations,” in “Advances in Neural Information Processing Systems” 2022.
- Han, Yufeng, Ai He, David Rapach, and Guofu Zhou**, “Expected stock returns and firm characteristics: E-LASSO, assessment, and implications,” *SSRN*, 2019.
- Harvey, Campbell R, Yan Liu, and Heqing Zhu**, “. . . and the cross-section of expected returns,” *The Review of Financial Studies*, 2016, *29* (1), 5–68.
- Hastie, Trevor, Andrea Montanari, Saharon Rosset, and Ryan J Tibshirani**, “Surprises in high-dimensional ridgeless least squares interpolation,” *Annals of statistics*, 2022, *50* (2), 949.
- Hou, Kewei, Chen Xue, and Lu Zhang**, “Replicating anomalies,” *The Review of Financial Studies*, 2020, *33* (5), 2019–2133.

- Hron, Jiri, Yasaman Bahri, Jascha Sohl-Dickstein, and Roman Novak**, “Infinite attention: NNGP and NTK for deep attention networks,” in “International Conference on Machine Learning” 2020.
- Jacot, Arthur, Franck Gabriel, and Clément Hongler**, “Neural tangent kernel: Convergence and generalization in neural networks,” *Advances in neural information processing systems*, 2018, 31.
- Jensen, Theis Ingerslev, Bryan Kelly, and Lasse Heje Pedersen**, “Is there a replication crisis in finance?,” *The Journal of Finance*, 2023, 78 (5), 2465–2518.
- Jumper, John, Richard Evans, Alexander Pritzel, Tim Green, Michael Figurnov, Olaf Ronneberger, Kathryn Tunyasuvunakool, Russ Bates, Augustin Žídek, Anna Potapenko et al.**, “Highly accurate protein structure prediction with AlphaFold,” *Nature*, 2021, 596 (7873), 583–589.
- Kelly, Bryan and Dacheng Xiu**, “Financial Machine Learning,” *Working Paper*, 2023.
- , **Seth Pruitt, and Yinan Su**, “Characteristics are Covariances: A Unified Model of Risk and Return,” *Journal of Financial Economics*, 2020.
- Kelly, Bryan T, Boris Kuznetsov, Semyon Malamud, and Teng Andrea Xu**, “Deep Learning from Implied Volatility Surfaces,” *Swiss Finance Institute Research Paper*, 2023, (23-60).
- , **Semyon Malamud, and Kangying Zhou**, “The Virtue of Complexity Everywhere,” *Available at SSRN*, 2022.
- , —, **Mohammad Pourmohammadi, and Fabio Trojani**, “Universal Portfolio Shrinkage,” *Swiss Finance Institute Research Paper*, 2023.
- Kingma, Diederik P and Jimmy Ba**, “Adam: A method for stochastic optimization,” *arXiv preprint arXiv:1412.6980*, 2014.
- Kozak, Serhiy**, “Kernel trick for the cross-section,” *Available at SSRN 3307895*, 2020.
- **and Stefan Nagel**, “When do cross-sectional asset pricing factors span the stochastic discount factor?,” Technical Report, National Bureau of Economic Research 2023.
- , —, **and Shrihari Santosh**, “Shrinking the cross-section,” *Journal of Financial Economics*, 2020, 135 (2), 271–292.
- , —, **and —**, “Shrinking the cross-section,” *Journal of Financial Economics*, 2020, 135 (2), 271–292.
- Kozak, Serhiy and Nagel**, “When do cross-sectional asset pricing factors span the stochastic discount factor?,” *Working Paper*, 2023.

- Lee, Jaehoon, Samuel Schoenholz, Jeffrey Pennington, Ben Adlam, Lechao Xiao, Roman Novak, and Jascha Sohl-Dickstein**, “Finite versus infinite neural networks: an empirical study,” *Advances in Neural Information Processing Systems*, 2020, *33*, 15156–15172.
- Leippold, Markus, Qian Wang, and Wenyu Zhou**, “Machine learning in the Chinese stock market,” *Journal of Financial Economics*, 2022, *145* (2), 64–82.
- Lettau, Martin and Markus Pelger**, “Factors that fit the time series and cross-section of stock returns,” *The Review of Financial Studies*, 2020, *33* (5), 2274–2325.
- McLean, R David and Jeffrey Pontiff**, “Does academic research destroy stock return predictability?,” *The Journal of Finance*, 2016, *71* (1), 5–32.
- Meng, Xuran, Jianfeng Yao, and Yuan Cao**, “Multiple descent in the multiple random feature model,” *arXiv preprint arXiv:2208.09897*, 2022.
- Merchant, Amil, Simon Batzner, Samuel S Schoenholz, Muratahan Aykol, Gowoon Cheon, and Ekin Dogus Cubuk**, “Scaling deep learning for materials discovery,” *Nature*, 2023, pp. 1–6.
- Moritz, Benjamin and Tom Zimmermann**, “Tree-based conditional portfolio sorts: The relation between past and future stock returns,” *Available at SSRN 2740751*, 2016.
- Nakkiran, Preetum, Gal Kaplun, Yamini Bansal, Tristan Yang, Boaz Barak, and Ilya Sutskever**, “Deep double descent: Where bigger models and more data hurt,” *Journal of Statistical Mechanics: Theory and Experiment*, 2021, *2021* (12), 124003.
- Novak, Roman, Jascha Sohl-Dickstein, and Samuel S. Schoenholz**, “Fast Finite Width Neural Tangent Kernel,” in “International Conference on Machine Learning” 2022.
- , **Lechao Xiao, Jiri Hron, Jaehoon Lee, Alexander A Alemi, Jascha Sohl-Dickstein, and Samuel S Schoenholz**, “Neural tangents: Fast and easy infinite neural networks in python,” *arXiv preprint arXiv:1912.02803*, 2019.
- , —, —, —, **Alexander A. Alemi, Jascha Sohl-Dickstein, and Samuel S. Schoenholz**, “Neural Tangents: Fast and Easy Infinite Neural Networks in Python,” in “International Conference on Learning Representations” 2020.
- Preite, Massimo Dello, Raman Uppal, Paolo Zaffaroni, and Irina Zviadadze**, “What is Missing in Asset-Pricing Factor Models?,” 2022.
- Rahimi, Ali and Benjamin Recht**, “Random Features for Large-Scale Kernel Machines.,” in “NIPS,” Vol. 3 Citeseer 2007, p. 5.
- Ross, Stephen A.**, “The Arbitrage Theory of Capital Asset Pricing,” *Journal of Economic Theory*, 1976, *13*, 341–360.

- Simon, Frederik, Sebastian Weibels, and Tom Zimmermann**, “Deep Parametric Portfolio Policies,” *Available at SSRN 4150292*, 2022.
- Sohl-Dickstein, Jascha, Roman Novak, Samuel S. Schoenholz, and Jaehoon Lee**, “On the infinite width limit of neural networks with a standard parameterization,” 2020.
- Yang, Greg**, “Tensor programs ii: Neural tangent kernel for any architecture,” *arXiv preprint arXiv:2006.14548*, 2020.
- and **Edward J Hu**, “Tensor programs iv: Feature learning in infinite-width neural networks,” in “International Conference on Machine Learning” PMLR 2021, pp. 11727–11737.
- , **Dingli Yu, Chen Zhu, and Soufiane Hayou**, “Tensor Programs VI: Feature Learning in Infinite-Depth Neural Networks,” *arXiv preprint arXiv:2310.02244*, 2023.
- Zhou, Yefan, Tianyu Pang, Keqin Liu, Charles H Martin, Michael W Mahoney, and Yaoqing Yang**, “Temperature Balancing, Layer-wise Weight Analysis, and Neural Network Training,” *arXiv preprint arXiv:2312.00359*, 2023.

A Proofs

A.1 Preliminaries on Gaussian Processes

- A Gaussian Process is a Gaussian distribution on **functions**.
- Basically, instead of randomly sampling a vector $f \in \mathbb{R}^P$, nature randomly samples a whole function $f(x) : \mathbb{R}^d \rightarrow \mathbb{R}$. Each value $x \in \mathbb{R}^d$ is a “coordinate” (thus, there is a continuum of coordinates)
- A Gaussian vector $f \in \mathbb{R}^P$ is defined by a $\mu, \Sigma : \mu(i) = E[f(i)], \Sigma(i, j) = \text{Cov}(f(i), f(j))$
- In a Gaussian process, we just replace coordinates $i, j = 1, \dots, P$ with variables $x_1, x_2 \in \mathbb{R}^d$. Thus, a Gaussian process (\mathcal{GP}) is defined by

$$\mu(x) = E[f(x)] \tag{80}$$

and

$$K(x, \tilde{x}) = E[f(x) f(\tilde{x})] \tag{81}$$

Here, K is the **covariance kernel of the Gaussian Process**

- The standard notation is: $f(x) \sim \mathcal{GP}(\mu(x), \Sigma(x))$, meaning that f is a Gaussian process with the mean $\mu(x)$ and the covariance kernel $\Sigma(x)$.
- Suppose now we are trying to learn a function $f(x)$ from many noisy observations

$$y_i = f(x_i) + \varepsilon_i, \varepsilon_i \sim N(0, \sigma_\varepsilon^2),$$

where ε_i are i.i.d. Gaussian, independent of $f(x_i)$ and of x_i . We can then use the **Gaussian conditioning formula**:

$$\begin{aligned} \begin{pmatrix} X \\ Y \end{pmatrix} &\sim N\left(\begin{pmatrix} \mu_X \\ \mu_Y \end{pmatrix}, \begin{pmatrix} \Sigma_{XX} & \Sigma_{XY} \\ \Sigma_{YX} & \Sigma_{YY} \end{pmatrix}\right) \\ E[X|Y] &= \mu_X + \Sigma_{XY}\Sigma_{YY}^{-1}(Y - \mu_Y) \\ \text{Var}[X|Y] &= \Sigma_{XX} - \Sigma_{XY}\Sigma_{YY}^{-1}\Sigma_{YX}. \end{aligned} \tag{82}$$

When applied to the Gaussian process, we get, with $Y = (y_1, \dots, y_n)$, that

$$\begin{pmatrix} f(x) \\ Y \end{pmatrix} \sim N\left(\begin{pmatrix} \mu(x) \\ \mu(X) \end{pmatrix}, \begin{pmatrix} K(x, x) & K(x, X) \\ K(X, x) & K(X, X) + \sigma_\varepsilon^2 I \end{pmatrix}\right) \tag{83}$$

and, hence

$$\begin{aligned} E[f(x)|(y_1, \dots, y_n)] &= \underbrace{\mu(x)}_{=E[f(x)]} + \underbrace{K(x, X)}_{=\text{Cov}(f(x), Y)} \underbrace{(\sigma_\varepsilon^2 I + K(X, X))^{-1}(Y - \mu(X))}_{\text{Var}[Y]^{-1}} \\ \text{Var}[f(x)|(y_1, \dots, y_n)] &= \underbrace{K(x, x)}_{=\text{Var}[f(x)]} - K(x, X) (\sigma_\varepsilon^2 I + K(X, X))^{-1} K(X, x) \end{aligned} \tag{84}$$

- If we have multiple OOS points X_{OOS} , we get that, from the **Bayesian point of view**, we have that

$$\text{Var}[f(X_{OOS})|(f(x_1), \dots, f(x_n))] = \underbrace{K(X_{OOS}, X_{OOS})}_{\text{ex-ante variance}} - \underbrace{K(X_{OOS}, X) (\sigma_\varepsilon^2 I + K(X, X))^{-1} K(X, X_{OOS})}_{\text{variance reduction}} \tag{85}$$

A.2 Neural Network Gaussian Process

In this section, for the readers' convenience, we present proof of the fact that, in the large width limit, the DNN at initialization is a Gaussian Process. In a slightly different form, this result is contained in (Jacot et al., 2018).

Theorem 8 *The function $f(x; \theta)$ in (33) in the limit of infinite width is a Gaussian process with mean zero and the covariance kernel $(\sigma_W^{(L)})^2 \Sigma^{(L)}(x, \tilde{x})$.*

Proof of Theorem 8. We prove the claim by induction. First, we notice that

$$z_i^{(l)}(x) = \frac{1}{n_l^{1/2}} \sum_j W_{ij}^{(l)} y_j^{(l)}(x) + b_i^{(l)} \quad (86)$$

is Gaussian conditional on $y_j^{(l)}(x)$. Namely,

$$z_i^{(l)}(x) \mid y^{(l)} \sim \mathcal{GP}(0, (\sigma^{(l)})_w^2 K^{(l)} + (\sigma^{(l)})_b^2),$$

where we have defined

$$K^{(l)}(x, \tilde{x}) = \frac{1}{n^{(l)}} \sum_i y_i^{(l)}(x) y_i^{(l)}(\tilde{x}). \quad (87)$$

Our second observation is that

$$K^{(l)}(x, \tilde{x}) = \frac{1}{n^{(l)}} \sum_i y_i^{(l)}(x) y_i^{(l)}(\tilde{x}) = \frac{1}{n^{(l)}} \sum_i \phi(z_i^{(l-1)}(x)) \phi(z_i^{(l-1)}(\tilde{x})). \quad (88)$$

Since

$$z_i^{(l-1)}(x) \mid y^{(l-1)} \sim \mathcal{GP}(0, (\sigma^{(l-1)})_w^2 K^{(l-1)} + (\sigma^{(l-1)})_b^2),$$

we get that

$$\lim_{n^{(l)} \rightarrow \infty} K^{(l)}(x, \tilde{x}) = \int dz d\tilde{z} \phi(z) \phi(\tilde{z}) \mathcal{N} \left(\begin{bmatrix} z \\ \tilde{z} \end{bmatrix}; \mathbf{0}, (\sigma^{(l-1)})_w^2 \begin{bmatrix} K^{(l-1)}(x, x) & K^{(l-1)}(x, \tilde{x}) \\ K^{(l-1)}(\tilde{x}, x) & K^{(l-1)}(\tilde{x}, \tilde{x}) \end{bmatrix} + (\sigma^{(l-1)})_b^2 \mathbf{1}_{2 \times 2} \right). \quad (89)$$

where $K^{(l-1)}$ is the finite width (and hence random) kernel. Now, sending $n_l \rightarrow \infty$ for all l implies that all kernels $K^{(l)}$ become constant and, hence, $z^{(l)}$ is a Gaussian process for each l . \square

A.3 The NTK in the Infinite Width Limit

Theorem 9 Suppose that $\phi(x)$ is uniformly Lipschitz.¹⁹ Then, at initialization,

$$\nabla_{\theta} z_i^{(l)}(x) \nabla_{\theta} z_{i_1}^{(l)}(\tilde{x}) \rightarrow \delta_{i,i_1} \Theta^{(l+1)}(x, \tilde{x}) \quad (90)$$

where Θ is defined in Definition 4.

Proof of Theorem 9. The proof is by induction. Recall that

$$\begin{aligned} x &= \text{input} \in \mathbb{R}^d \\ y^{(l)}(x) &= \begin{cases} x & \text{if } l = 0, \\ \phi(z^{(l-1)}(x)) & \text{if } l > 0. \end{cases} \\ z_i^{(l)}(x) &= \frac{1}{n_l^{1/2}} \sum_j W_{ij}^{(l)} y_j^{(l)}(x) + b_i^{(l)}, \end{aligned} \quad (91)$$

where $y^{(l)}(x), z^{(l-1)}(x) \in \mathbb{R}^{n^{(l)} \times 1}$. We have

$$z_i^{(0)}(x) = \frac{1}{n_0^{1/2}} \sum_{j=1}^{n_0} W_{i,j}^{(0)} x_j + b_j^0 \quad (92)$$

and, hence,

$$\nabla_{\theta} z_i^{(0)}(x) = \left(\frac{1}{n_0^{1/2}} x, 1 \right), \quad (93)$$

so that

$$\nabla_{\theta} z_i^{(0)}(x) \nabla_{\theta} z_{i_1}^{(0)}(\tilde{x})' = \delta_{i,i_1} \left(\frac{1}{n_0} x' \tilde{x} + 1 \right) = \delta_{i,i_1} (\Sigma^{(1)}(x, \tilde{x}) + 1) = \delta_{i,i_1} \Theta^{(1)}(x, \tilde{x}). \quad (94)$$

We now proceed by induction. Suppose we have proved the claim for $z^{(l-1)}$. We have

$$z_i^{(l)}(x) = \frac{1}{n_l^{1/2}} \sum_{j=1}^{n_l} W_{i,j}^{(l)} \phi(z_j^{(l-1)}(x)) + b_i^{(l)} \quad (95)$$

The vector of coefficients of this neural network, θ , can be decomposed into $\theta = (\theta_{l-1}, W^{(l)}, b^{(l)})$, where θ_{l-1} are all the coefficients except for those of the l 'th layer. Each $z_j^{(l)}(x), j = 1, \dots, n_l$.

¹⁹That is, $|\phi(x) - \phi(y)| \leq C|x - y|$ for some $C > 0$.

We have

$$\begin{aligned}
\nabla_{\theta_{l-1} z_i^{(l)}}(x) &= \frac{1}{n_l^{1/2}} \sum_{j=1}^{n_l} W_{i,j}^{(l)} \nabla_{\theta_{l-1}} \phi(z_j^{(l-1)}(x)) \\
&= \frac{1}{n_l^{1/2}} \sum_{j=1}^{n_l} W_{i,j}^{(l)} \nabla_{\theta_{l-1}} z_j^{(l-1)}(x) \phi'(z_j^{(l-1)}(x))
\end{aligned} \tag{96}$$

and, hence,

$$\begin{aligned}
&\nabla_{\theta_{l-1} z_{i_1}^{(l)}}(x) \nabla_{\theta_{l-1} z_{i_2}^{(l)}}(\tilde{x})' \\
&= \frac{1}{n_l} \sum_{j_1=1}^{n_l} W_{i_1,j_1}^{(L+1)} \nabla_{\theta_{l-1}} z_{j_1}^{(l-1)}(x) \phi'(z_{j_1}^{(l-1)}(x)) \sum_{j_2=1}^{n_l} W_{i_2,j_2}^{(l)} \nabla_{\theta_{l-1}} z_{j_2}^{(l-1)}(\tilde{x}) \phi'(z_{j_2}^{(l-1)}(\tilde{x})).
\end{aligned} \tag{97}$$

By the induction hypothesis, in the limit as $n_{l-1}, \dots, n_1 \rightarrow \infty$, we have

$$\begin{aligned}
&\nabla_{\theta_{l-1} z_{i_1}^{(l)}}(x) \nabla_{\theta_{l-1} z_{i_2}^{(l)}}(\tilde{x})' \\
&\approx \frac{1}{n_l} \sum_{j_1=1}^{n_l} W_{i_1,j_1}^{(L+1)} \phi'(z_{j_1}^{(l-1)}(x)) \sum_{j_2=1}^{n_l} W_{i_2,j_2}^{(l)} \phi'(z_{j_2}^{(l-1)}(\tilde{x})) \delta_{j_1,j_2} \Theta^{(l)}(x, \tilde{x}) \\
&= \frac{1}{n_l} \sum_{j=1}^{n_l} W_{i_1,j}^{(L+1)} \phi'(z_j^{(l-1)}(x)) W_{i_2,j}^{(l)} \phi'(z_j^{(l-1)}(\tilde{x})) \Theta^{(l)}(x, \tilde{x})
\end{aligned} \tag{98}$$

In the limit as $n_l \rightarrow \infty$, we get

$$\begin{aligned}
&\nabla_{\theta_{l-1} z_{i_1}^{(l)}}(x) \nabla_{\theta_{l-1} z_{i_2}^{(l)}}(\tilde{x})' \\
&\rightarrow \delta_{i_1,i_2} (\sigma_W^{(l)})^2 E[\phi'(z_j^{(l-1)}(x)) \phi'(z_j^{(l-1)}(\tilde{x}))] \Theta^{(l)}(x, \tilde{x})
\end{aligned} \tag{99}$$

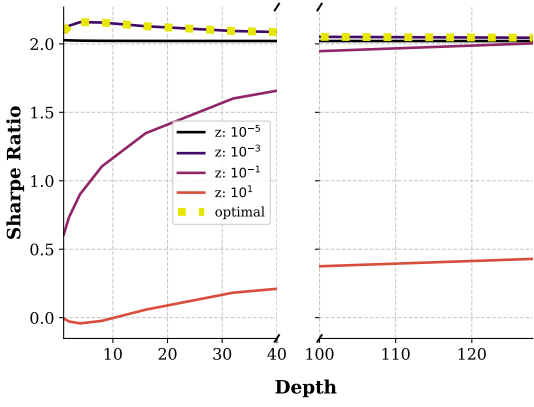
At the same time,

$$\begin{aligned}
&\nabla_{(W^{(l)}, b^{(l)}) z_{i_1}^{(l)}}(x) \nabla_{(W^{(l)}, b^{(l)}) z_{i_2}^{(l)}}(\tilde{x})' \\
&= \delta_{i_1,i_2} \left(\frac{1}{n_l} \sum_j \phi(z_j^{(l-1)}(x)) \phi(z_j^{(l-1)}(\tilde{x})) + 1 \right) \\
&\rightarrow \delta_{i_1,i_2} (E[\phi(z_j^{(l-1)}(x)) \phi(z_j^{(l-1)}(\tilde{x}))] + 1) \\
&= \delta_{i_1,i_2} (\Sigma^{(l)}(x, \tilde{x}) + 1)
\end{aligned} \tag{100}$$

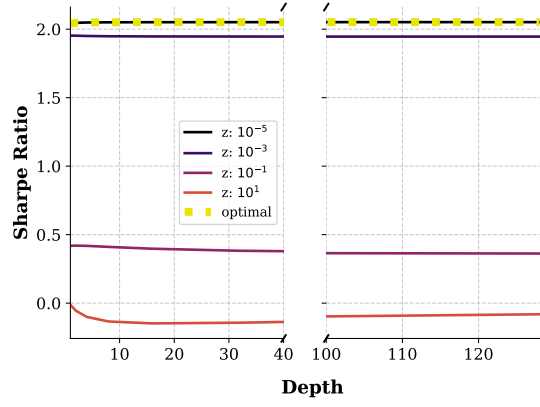
□

Theorem 10

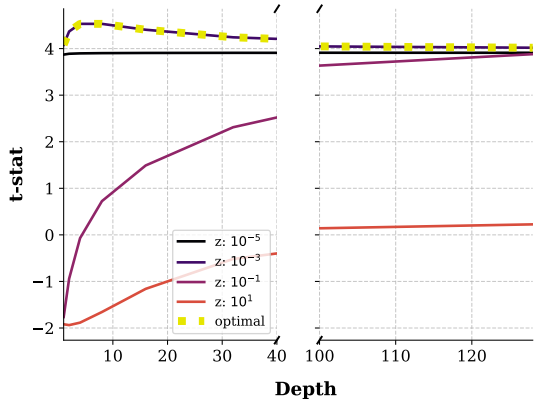
B Results



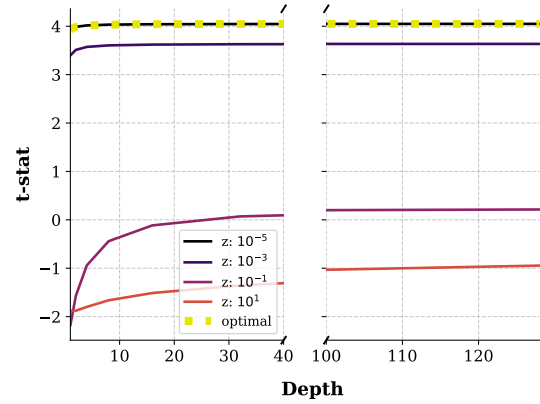
(a) Sharpe ratio, NTK



(b) Sharpe ratio, NNGP

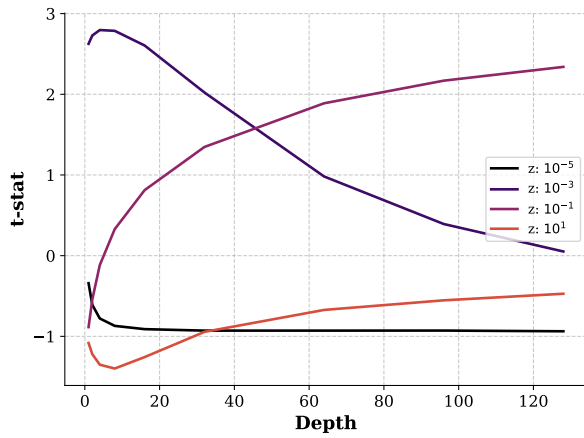


(c) Alpha t-statistic, NTK

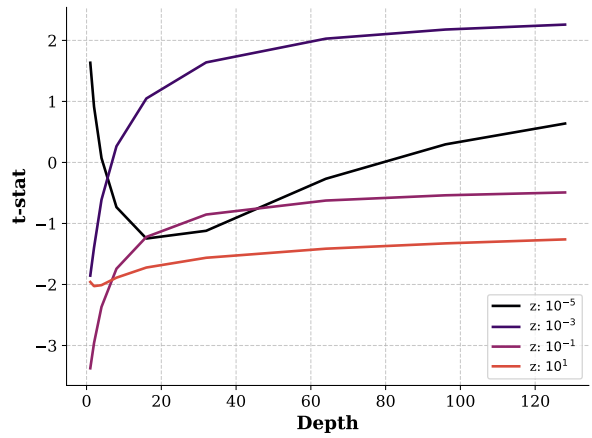


(d) Alpha t-statistic, NNGP

Figure 2: $RW=12$, $act=ReLU$, $\alpha=0.5$. The figure above presents Sharpe ratios and t-statistics of alpha intercepts for the NTK and NNGP kernel portfolios from 1993/03 to 2022/11 as functions of the depth of the neural network underlying the kernels for various values of shrinkage parameters z . NTK stands for the NTK kernel portfolio, and NNGP stands for the NNGP kernel portfolio. Depth is the number of inner layers of the neural network. The t-statistics for alpha intercepts are derived from OLS regressions of the monthly returns of NTK (NNGP) kernel portfolios on Fama-French factors and the complexity factor. Fama-French factors include $R_m - R_f$, HML, SMB, Monthly 2-12 Momentum, Short-Term and Long-Term Reversal (as described in Kenneth R. French data library).

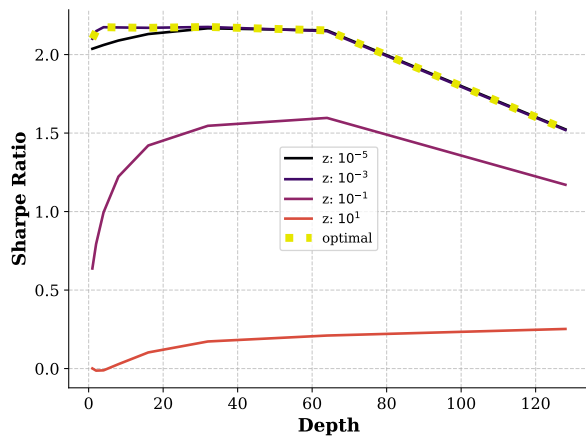


(a) Alpha t-statistic, NTK over NNGP

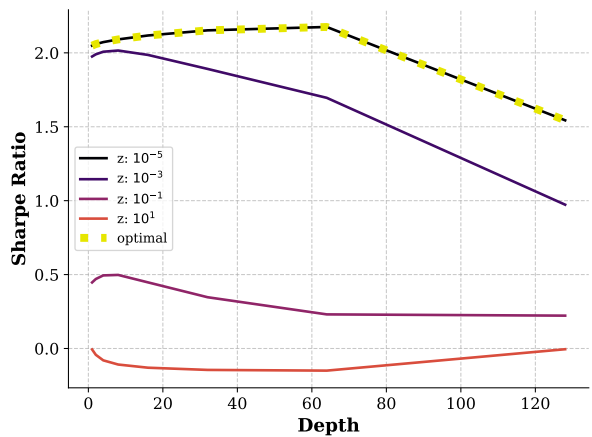


(b) Alpha t-statistic, NNGP over NTK

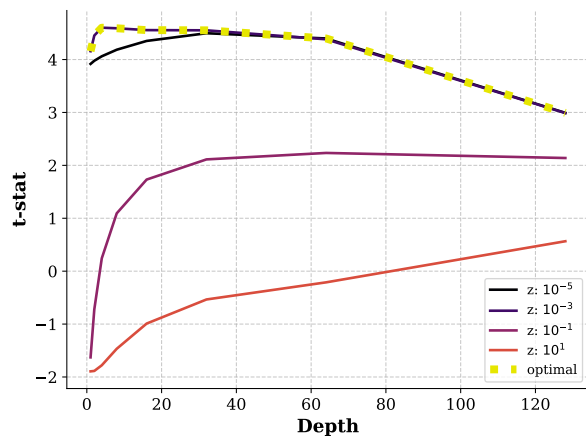
Figure 3: RW=12, act=ReLU, $\alpha=0.5$. The figure above shows t-statistics of alpha intercepts for the NTK (NNGP) kernel portfolio with respect to the NNGP (NTK) kernel portfolio from 1993/03 to 2022/11 as functions of the depth of the neural network underlying the kernels for various values of shrinkage parameters z . NTK stands for the NTK kernel portfolios, and NNGP stands for the NNGP kernel portfolios. Depth is the number of inner layers of the neural network.



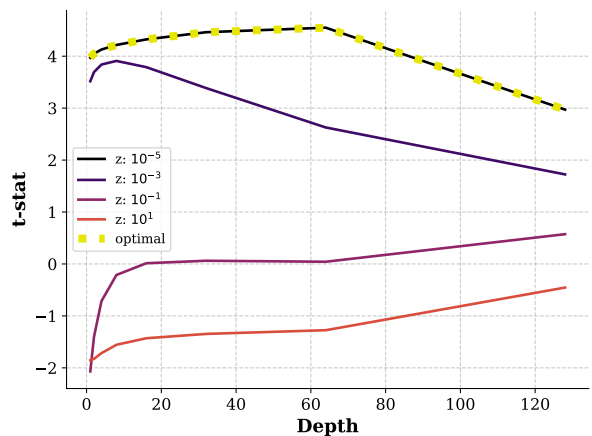
(a) Sharpe ratio, NTK



(b) Sharpe ratio, NNGP

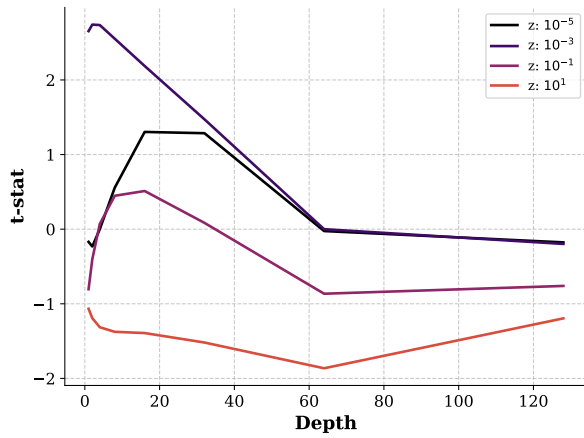


(c) Alpha t-statistic, NTK

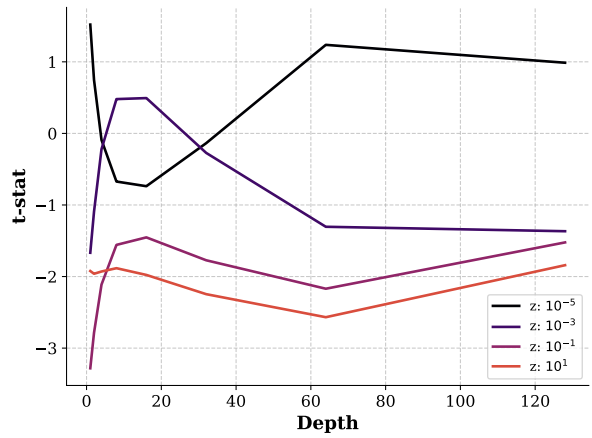


(d) Alpha t-statistic, NNGP

Figure 4: $RW=12$, $act=Erf$, $\alpha=0.5$. The figure above presents Sharpe ratios and t-statistics of alpha intercepts for the NTK and NNGP kernel portfolios from 1993/03 to 2022/11 as functions of the depth of the neural network underlying the kernels for various values of shrinkage parameters z . NTK stands for the NTK kernel portfolio, and NNGP stands for the NNGP kernel portfolio. Depth is the number of inner layers of the neural network. The t-statistics for alpha intercepts are derived from OLS regressions of the monthly returns of NTK (NNGP) kernel portfolios on Fama-French factors and the complexity factor. Fama-French factors include $R_m - R_f$, HML, SMB, Monthly 2-12 Momentum, Short-Term and Long-Term Reversal (as described in Kenneth R. French data library).

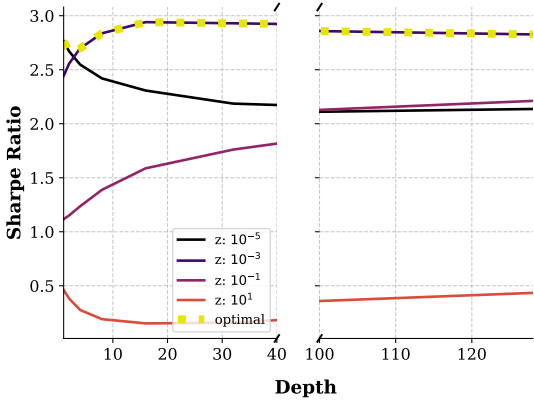


(a) Alpha t-statistic, NTK over NNGP

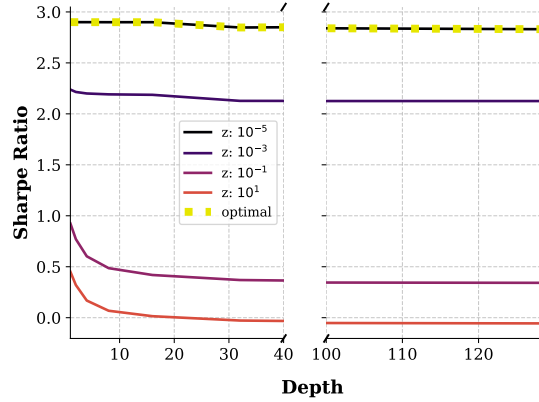


(b) Alpha t-statistic, NNGP over NTK

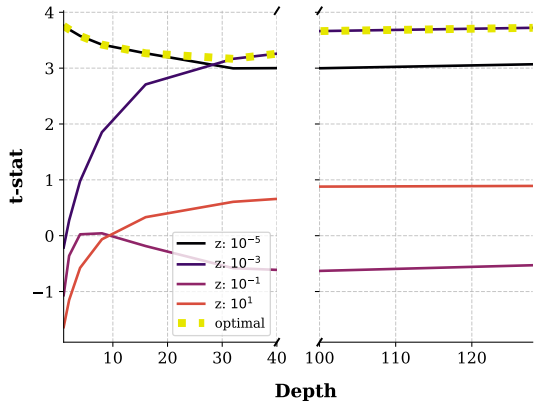
Figure 5: $RW=12$, $act=Erf$, $\alpha=0.5$. The figure above shows t-statistics of alpha intercepts for the NTK (NNGP) kernel portfolio with respect to the NNGP (NTK) kernel portfolio from 1993/03 to 2022/11 as functions of the depth of the neural network underlying the kernels for various values of shrinkage parameters z . NTK stands for the NTK kernel portfolios, and NNGP stands for the NNGP kernel portfolios. Depth is the number of inner layers of the neural network.



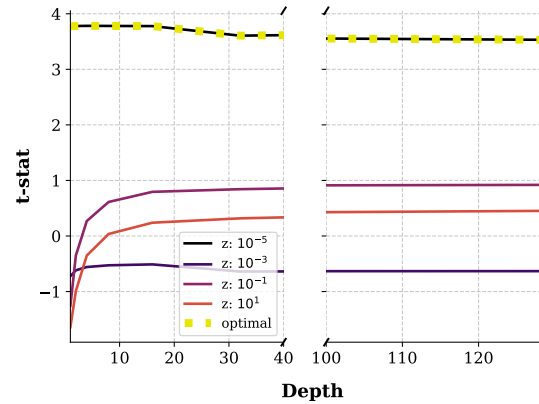
(a) Sharpe ratio, NTK



(b) Sharpe ratio, NNGP

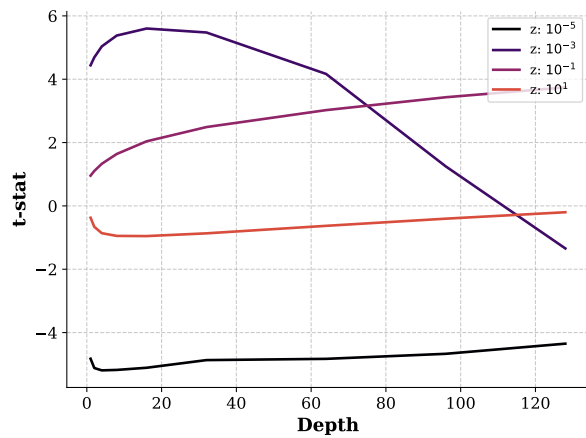


(c) Alpha t-statistic, NTK

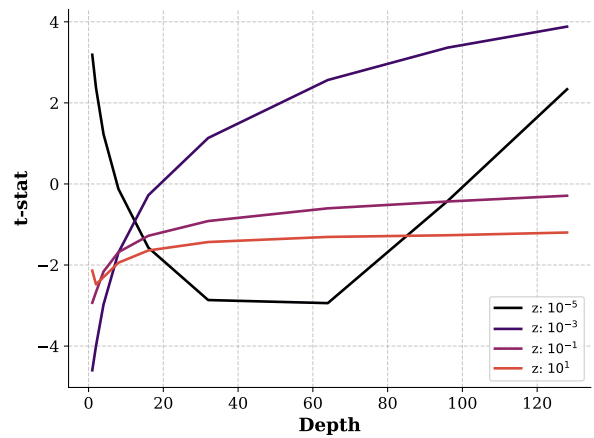


(d) Alpha t-statistic, NNGP

Figure 6: $RW=60$, $act=ReLU$, $\alpha=0.5$. The figure above presents Sharpe ratios and t-statistics of alpha intercepts for the NTK and NNGP kernel portfolios from 1993/03 to 2022/11 as functions of the depth of the neural network underlying the kernels for various values of shrinkage parameters z . NTK stands for the NTK kernel portfolio, and NNGP stands for the NNGP kernel portfolio. Depth is the number of inner layers of the neural network. The t-statistics for alpha intercepts are derived from OLS regressions of the monthly returns of NTK (NNGP) kernel portfolios on Fama-French factors and the complexity factor. Fama-French factors include $R_m - R_f$, HML, SMB, Monthly 2-12 Momentum, Short-Term and Long-Term Reversal (as described in Kenneth R. French data library).

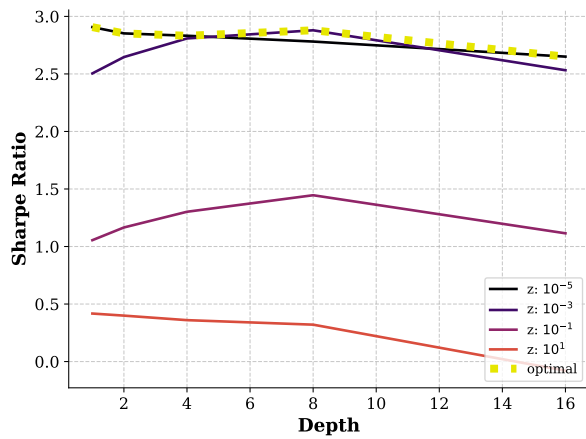


(a) Alpha t-statistic, NTK over NNGP

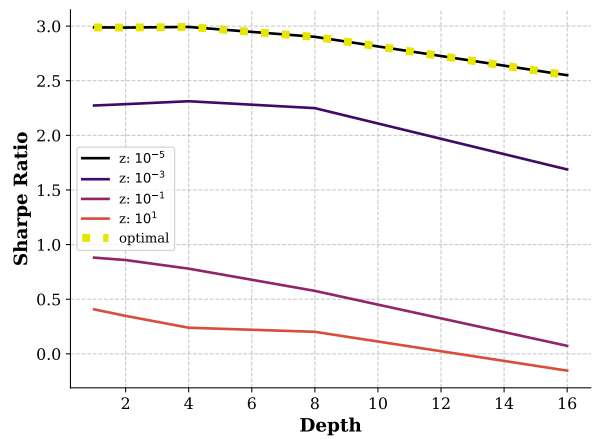


(b) Alpha t-statistic, NNGP over NTK

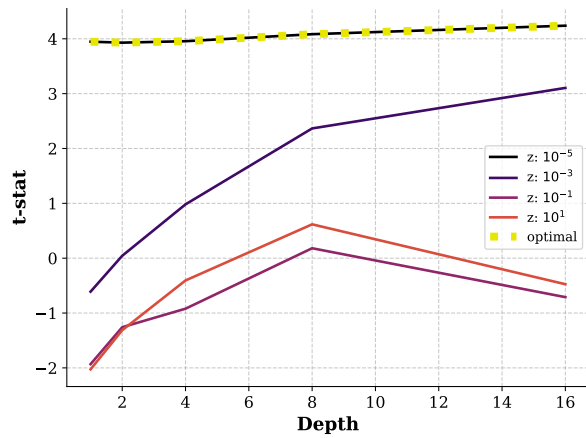
Figure 7: RW=60, act=ReLU, $\alpha=0.5$. The figure above shows t-statistics of alpha intercepts for the NTK (NNGP) kernel portfolio with respect to the NNGP (NTK) kernel portfolio from 1993/03 to 2022/11 as functions of the depth of the neural network underlying the kernels for various values of shrinkage parameters z . NTK stands for the NTK kernel portfolios, and NNGP stands for the NNGP kernel portfolios. Depth is the number of inner layers of the neural network.



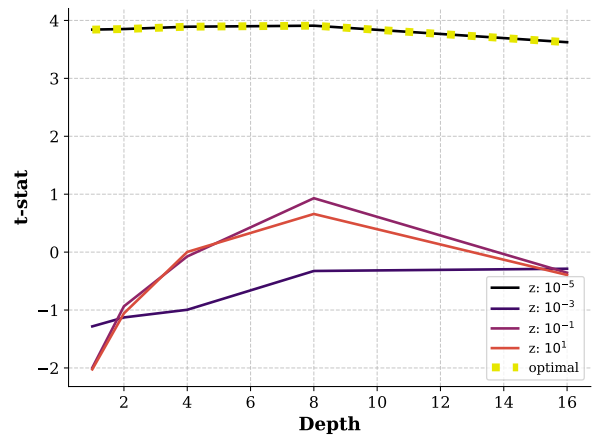
(a) Sharpe ratio, NTK



(b) Sharpe ratio, NNGP

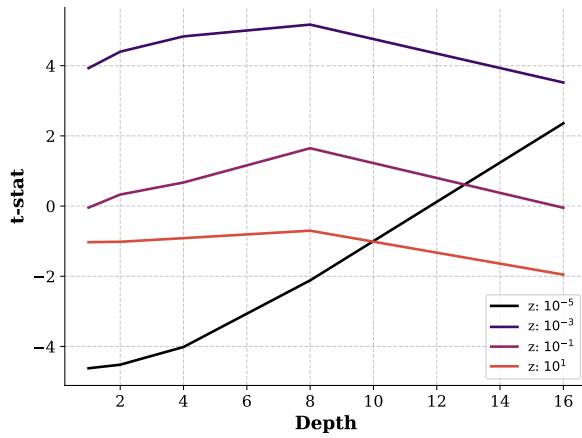


(c) Alpha t-statistic, NTK

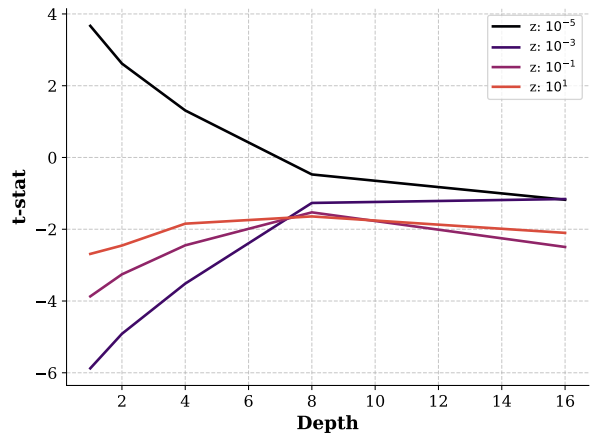


(d) Alpha t-statistic, NNGP

Figure 8: RW=60, act=Erf, $\alpha=0.5$. The figure above presents Sharpe ratios and t-statistics of alpha intercepts for the NTK and NNGP kernel portfolios from 1993/03 to 2022/11 as functions of the depth of the neural network underlying the kernels for various values of shrinkage parameters z . NTK stands for the NTK kernel portfolio, and NNGP stands for the NNGP kernel portfolio. Depth is the number of inner layers of the neural network. The t-statistics for alpha intercepts are derived from OLS regressions of the monthly returns of NTK (NNGP) kernel portfolios on Fama-French factors and the complexity factor. Fama-French factors include $R_m - R_f$, HML, SMB, Monthly 2-12 Momentum, Short-Term and Long-Term Reversal (as described in Kenneth R. French data library).

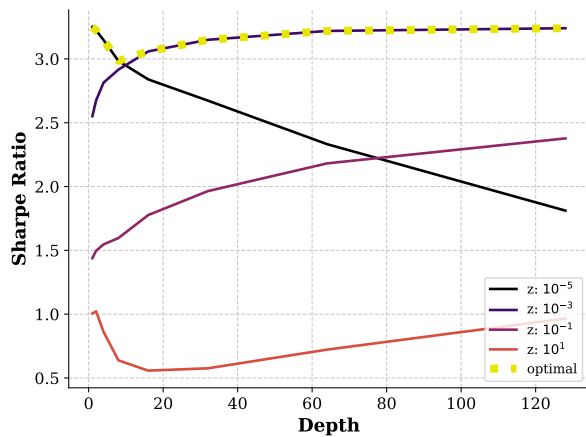


(a) Alpha t-statistic, NTK over NNGP

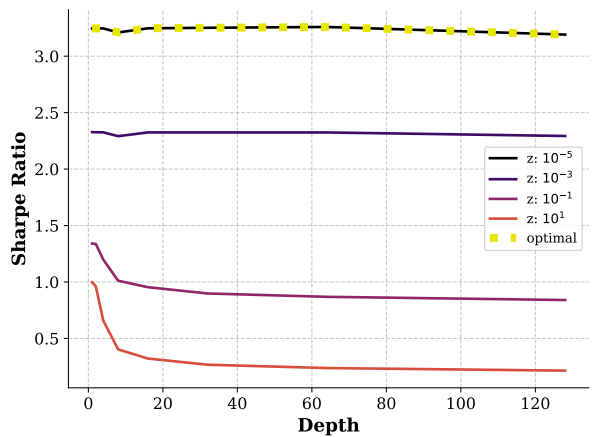


(b) Alpha t-statistic, NNGP over NTK

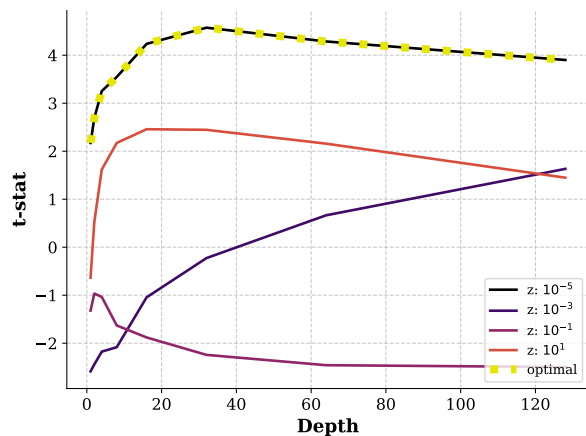
Figure 9: RW=60, act=Erf, $\alpha=0.5$. The figure above shows t-statistics of alpha intercepts for the NTK (NNGP) kernel portfolio with respect to the NNGP (NTK) kernel portfolio from 1993/03 to 2022/11 as functions of the depth of the neural network underlying the kernels for various values of shrinkage parameters z . NTK stands for the NTK kernel portfolios, and NNGP stands for the NNGP kernel portfolios. Depth is the number of inner layers of the neural network.



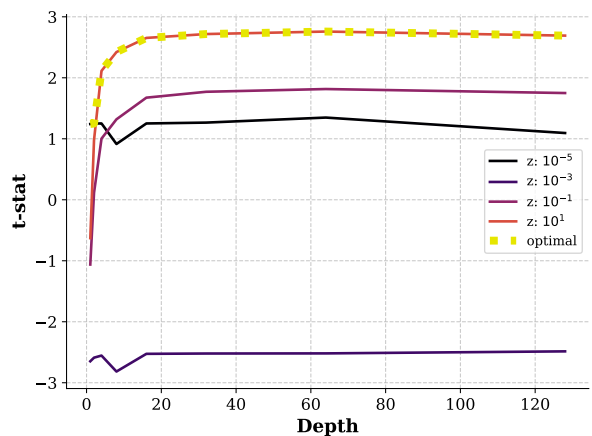
(a) Sharpe ratio, NTK



(b) Sharpe ratio, NNGP

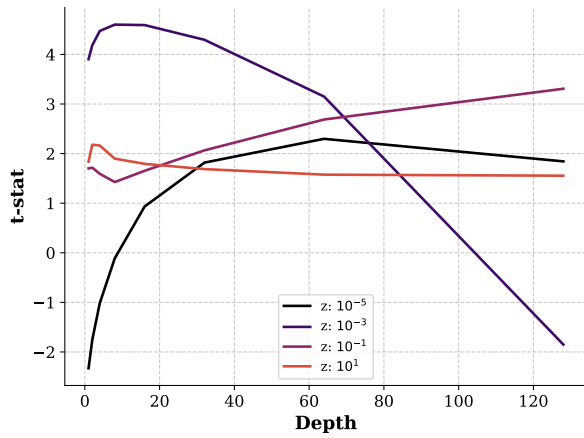


(c) Alpha t-statistic, NTK

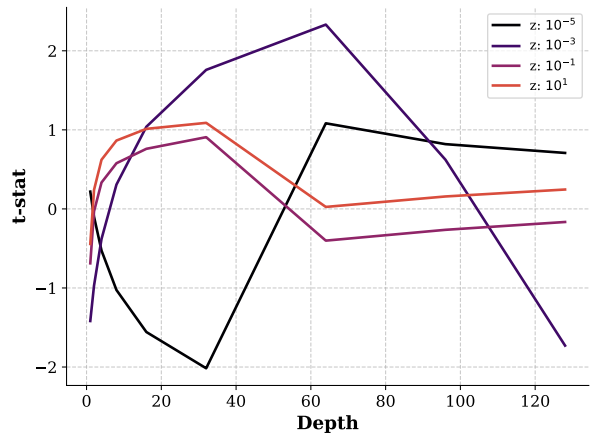


(d) Alpha t-statistic, NNGP

Figure 10: RW=120, act=ReLU, $\alpha=0.5$. The figure above presents Sharpe ratios and t-statistics of alpha intercepts for the NTK and NNGP kernel portfolios from 1993/03 to 2022/11 as functions of the depth of the neural network underlying the kernels for various values of shrinkage parameters z . NTK stands for the NTK kernel portfolio, and NNGP stands for the NNGP kernel portfolio. Depth is the number of inner layers of the neural network. The t-statistics for alpha intercepts are derived from OLS regressions of the monthly returns of NTK (NNGP) kernel portfolios on Fama-French factors and the complexity factor. Fama-French factors include $R_m - R_f$, HML, SMB, Monthly 2-12 Momentum, Short-Term and Long-Term Reversal (as described in Kenneth R. French data library).



(a) Alpha t-statistic, NTK over NNGP



(b) Alpha t-statistic, NNGP over NTK

Figure 11: $RW=120$, $act=ReLU$, $\alpha=0.5$. The figure above shows t-statistics of alpha intercepts for the NTK (NNGP) kernel portfolio with respect to the NNGP (NTK) kernel portfolio from 1993/03 to 2022/11 as functions of the depth of the neural network underlying the kernels for various values of shrinkage parameters z . NTK stands for the NTK kernel portfolios, and NNGP stands for the NNGP kernel portfolios. Depth is the number of inner layers of the neural network.